

Special Section:

The Arctic: An AGU Joint
Special Collection

†Deceased 15 April 2022.

Key Points:

- Multiyear sea ice (MYI) loss from the Arctic Ocean has primarily occurred through two stepwise reductions: 1989 and 2006–2008
- 1989 was the result of high MYI export, while 2006–2008 was the result of high MYI export and melt, and limited MYI replenishment
- Though presently stable, reduced retention to older MYI has created a younger thinner MYI pack that may be conditioned for another reduction

Supporting Information:

Supporting Information may be found in
the online version of this article.

Correspondence to:

D. G. Babb,
david.babb@umanitoba.ca









Citation:

Babb, D. G., Galley, R. J., Kirillov, S.,
Landy, J. C., Howell, S. E. L., Stroeve,
J. C., et al. (2023). The stepwise
reduction of multiyear sea ice area in
the Arctic Ocean since 1980. *Journal
of Geophysical Research: Oceans*,
128, e2023JC020157. [https://doi.
org/10.1029/2023JC020157](https://doi.org/10.1029/2023JC020157)

Received 20 JUN 2023

Accepted 22 SEP 2023

© 2023. The Authors.

This is an open access article under
the terms of the [Creative Commons
Attribution License](#), which permits use,
distribution and reproduction in any
medium, provided the original work is
properly cited.The Stepwise Reduction of Multiyear Sea Ice Area in the
Arctic Ocean Since 1980D. G. Babb^{1,2} , R. J. Galley^{2,3} , S. Kirillov¹ , J. C. Landy⁴ , S. E. L. Howell⁵ ,
J. C. Stroeve^{1,2,6,7} , W. Meier⁷ , J. K. Ehn^{1,2} , and D. G. Barber^{1,2,†}¹Centre for Earth Observation Science, University of Manitoba, Winnipeg, MB, Canada, ²Department of Environment and Geography, University of Manitoba, Winnipeg, MB, Canada, ³Department of Fisheries and Oceans Canada, Winnipeg, MB, Canada, ⁴Department of Physics and Technology, UiT The Arctic University of Norway, Tromsø, Norway, ⁵Environment and Climate Change Canada, Toronto, ON, Canada, ⁶Department of Earth Sciences, University College London, London, UK, ⁷National Snow and Ice Data Center, Cooperative Institute for Research in Environmental Sciences at the University of Colorado Boulder, Boulder, CO, USA

Abstract The loss of multiyear sea ice (MYI) in the Arctic Ocean is a significant change that affects all facets of the Arctic environment. Using a Lagrangian ice age product, we examine MYI loss and quantify the annual MYI area budget from 1980 to 2021 as the balance of export, melt, and replenishment. Overall, MYI area declined at 72,500 km²/yr; however, a majority of the loss occurred during two stepwise reductions that interrupt an otherwise balanced budget and resulted in the northward contraction of the MYI pack. First, in 1989, a change in atmospheric forcing led to a +56% anomaly in MYI export through Fram Strait. The second occurred from 2006 to 2008 with anomalously high melt (+25%) and export (+23%) coupled with low replenishment (−8%). In terms of trends, melt has increased since 1989, particularly in the Beaufort Sea, export has decreased since 2008 due to reduced MYI coverage north of Fram Strait, and replenishment has increased over the full time series due to a negative feedback that promotes seasonal ice survival at higher latitudes exposed by MYI loss. However, retention of older MYI has significantly declined, transitioning the MYI pack toward younger MYI that is less resilient than previously anticipated and could soon elicit another stepwise reduction. We speculate that future MYI loss will be driven by increased melt and reduced replenishment, both of which are enhanced with continued warming and will one day render the Arctic Ocean free of MYI, a change that will coincide with a seasonally ice-free Arctic Ocean.

Plain Language Summary Sea ice that has survived through at least one melt season is referred to as multiyear sea ice. It is inherently thicker, has a higher albedo and is overall more resilient to melt than seasonal sea ice. Historically, multiyear ice covered a vast majority of the Arctic Ocean, however its areal extent has declined and transitioned the Arctic ice pack to a younger state that is more susceptible to melt. To this point, the loss of multiyear ice is known, but it remains unclear whether it was a change in multiyear ice loss through export or melt or the source of multiyear through replenishment that has driven this change. By quantifying these three terms for each of the past 42 years, we find that multiyear ice loss primarily occurred through two stepwise reductions, with the budget otherwise generally being in balance. The first loss occurred in 1989 due to anomalously high export, while the second loss occurred between 2006 and 2008 through a confluence of anomalously high export and melt and low replenishment. Trends of reduced export, increased melt and increased replenishment, and overall negative multiyear ice balance, suggest the eventual disappearance of multiyear ice from the Arctic Ocean.

1. Introduction

The loss of multiyear sea ice (MYI) and transition to a predominantly first-year sea ice (FYI) cover is one of the most dramatic changes taking place in a warming Arctic (Comiso, 2012; Constable et al., 2022; Kwok, 2018; Maslanik et al., 2011; Meier et al., 2021; Meredith et al., 2019; Nghiem et al., 2011; Stroeve & Notz, 2018; Tschudi et al., 2016). MYI is defined as sea ice that has survived at least one melt season and ages as it survives through additional melt seasons. MYI is inherently thicker than FYI due to accumulated deformation and continued thermodynamic ice growth (Kwok, 2004a), and it has a higher albedo due to greater snow accumulation, a surface scattering layer and reduced melt pond coverage (Perovich & Polashenski, 2012). As a result, MYI is more robust and resilient to summer melt than FYI, and thus forms the backbone of the Arctic ice pack through

the melt season with the end of winter MYI edge being a prognosticator of the annual minimum sea ice extent (Thomas & Rothrock, 1993). As the Arctic has warmed, the MYI pack has declined in area (Comiso, 2012; Kwok, 2018; Maslanik et al., 2011) and thickness (Kacimi & Kwok, 2022; Kwok et al., 2009; Petty et al., 2023) weakening the backbone of the Arctic ice pack and making it more susceptible to further reductions. MYI loss represents a significant shift in the Arctic environment that has implications for the Arctic ecosystem, the global climate system, industrial and transportation related interests in the north, and most importantly for Inuit who live in the Arctic and rely on the marine environment (Constable et al., 2022; Meredith et al., 2019).

Historically, MYI covered a vast majority of the Arctic Ocean. A portion was exported annually through Fram Strait via the Transpolar Drift Stream while the majority was redistributed and retained within the Beaufort Gyre for more than 10 years (Rigor & Wallace, 2004). In the 1950s and 1960s, the end-of-winter MYI extent was approximately 5.5×10^6 km² (Nghiem et al., 2007). Beginning in the 1970s, the end-of-winter MYI extent decreased at a rate of 0.5×10^6 km² per decade and fell to approximately 4×10^6 km² by the end of the 20th century (Nghiem et al., 2007). MYI loss accelerated through the 2000s (Comiso, 2012) with a dramatic reduction in MYI area of 1.54×10^6 km² between 2005 and 2008 (Kwok et al., 2009), and a current record minimum of 1.6×10^6 km² at the end-of-winter 2017 (Kwok, 2018). Despite significant negative linear trends in MYI area, Comiso (2012) found an 8–9 years cycle in MYI area, with years of loss followed by recovery. Similarly, Regan et al. (2023) found that between 2000 and 2018 modeled MYI area declined through episodic losses in 2007 and 2012.

The reduction in MYI area coincides with the reduction in Arctic sea ice thickness that has occurred since the original observations of thickness were collected beneath a primarily MYI cover by submarines in the 1950s and 1960s (Bourke & Garret, 1987; Kwok & Rothrock, 2009; Rothrock et al., 1999). Ice thickness and age have been found to be positively correlated, with thickness increasing between 0.19 m (Maslanik et al., 2007) and 0.36 m (Tschudi et al., 2016) for every year that the ice ages. As a result, from 2003 to 2018, MYI area and winter sea ice volume were strongly correlated ($R^2 = 0.85$; Kwok, 2018). Overall, the reduction in MYI area has strongly contributed to the reduction in sea ice thickness within the Arctic Ocean.

Annual changes in MYI area within the Arctic Ocean reflect a balance between MYI loss through export, melt and deformation, and replenishment, which is FYI that survives through the melt season and is the sole source of MYI. Due to the limitations with quantifying MYI deformation, and the assumption that it is a relatively small term, we focus on the other three terms. To-date MYI export, replenishment, and melt have been examined in different works over different periods of time and for different regions (i.e., Babb et al., 2022; Howell et al., 2023; Kuang et al., 2022; Kwok, 2004b, 2007, 2009; Kwok & Cunningham, 2010; Kwok et al., 2009; Ricker et al., 2018), yet they have not been coherently analyzed to produce a long-term MYI budget of the Arctic Ocean and examine MYI loss. Regan et al. (2023) recently examined MYI area and volume loss from 2000 to 2018 in terms of MYI export, melt, replenishment, and ridging using the neXtSIM ice-ocean model, yet the model performs poorly during some years (i.e., 2016; Boutin et al., 2023) and is limited to an 18 year period at which point MYI had already declined considerably. In this paper, we use 43 years of remotely sensed fields of sea ice motion, age, and concentration to examine the MYI area budget of the Arctic Ocean. We use the relative changes and contributions of export, melt, and replenishment to understand what has driven the dramatic loss of MYI and what the future holds for MYI in the Arctic Ocean.

2. Background of the MYI Budget Terms

2.1. MYI Export

MYI can be exported across any of the open boundaries of the Arctic Ocean, though it is primarily exported through Fram Strait (87%; Kuang et al., 2022). A lesser amount is exported seasonally into Nares Strait (Howell et al., 2023; Kwok, 2005; Kwok et al., 2010; Moore, Howell, Brady, et al., 2021) and into the Queen Elizabeth Islands (QEI) of the CAA (Howell & Brady, 2019; Howell et al., 2023), while MYI has occasionally been exported into the Barents Sea (Kwok et al., 2005) and through the Bering Strait (Babb et al., 2013).

Estimates of annual total ice (MYI and FYI) area export through Fram Strait vary from 706,000 km² (Kwok, 2009) to 880,000 km² (Smedsrud et al., 2017), yet the proportion of MYI varies according to the orientation of the Transpolar Drift Stream, which advects sea ice toward Fram Strait. An eastward shift in the Transpolar Drift Stream results in more FYI export from the Russian Seas, whereas a westward shift results in older ice being more

readily drawn out of the Beaufort Gyre (Hansen et al., 2013; Kwok, 2009; Pfirman et al., 2004). The orientation of the Transpolar Drift Stream is dictated by the surface pressure patterns over the Arctic Ocean that is characterized by the Arctic Oscillation (AO) index. The negative phase of the AO shifts the Transpolar Drift Stream to the east, while the positive phase shifts the Transpolar Drift Stream to the west (Rigor et al., 2002). The shift from a prolonged negative AO to a positive AO in the late 1980s led to a “flushing” of MYI out of the Beaufort Gyre into the Transpolar Drift Stream and through Fram Strait (Pfirman et al., 2004). This flushing event is thought to have caused a permanent shift in the thickness and concentration of the Arctic ice pack (Lindsay & Zhang, 2005), a shift which ultimately conditioned it for the record minimum of 2007 (Lindsay et al., 2009).

In terms of the proportion of MYI passing through Fram Strait, Gow and Tucker (1987) reported that 84% of the ice in Fram Strait during the summer 1984 was MYI, while Kwok and Cunningham (2015) assumed 70% during winters (October–April) 2011–2014. More recently, Ricker et al. (2018) used the sea ice type product (OSI-403) from the EUMETSAT Ocean and Sea Ice Satellite Application Facility to estimate an MYI proportion between 64% and 94% during winters 2010–2017. Using the estimate of 706,000 km² of total ice export and the range in MYI proportion presented by Ricker et al. (2018), Babb et al. (2022) estimated that 453,000–660,000 km² of MYI was exported annually through Fram Strait. More recently, Wang et al. (2022) used another remotely sensed ice-type product (ECICE; Shokr et al., 2008) to determine that on average 343,000 km² of MYI was exported through Fram Strait during winter between 2002 and 2020. Given that approximately 87% of the annual total ice export through Fram Strait occurs during winter (Kwok, 2009), we assume that MYI export follows the annual cycle of total ice export and scale the results of Wang et al. (2022) to an annual average MYI export of 388,000 km². However, Wang et al. (2022) note that MYI export through Fram Strait declined by 22% between the first and second half of their study period, due to a reduction in MYI transport from the Beaufort Sea and Siberian coast toward Fram Strait and therefore younger ice in the Transpolar Drift Stream (i.e., Comiso, 2012; Haas et al., 2008; Hansen et al., 2013; Krumpfen et al., 2019; Sumata et al., 2023). Reduced MYI export aligns with the observed decrease in sea ice volume export through Fram Strait since the 1990s (Sumata et al., 2022).

MYI export into Nares Strait and the QEI is an order of magnitude lower than MYI export through Fram Strait, yet export is increasing through both channels. This is particularly important because the oldest and thickest MYI in the Arctic is exported through these channels (Howell et al., 2023; Kwok et al., 2010; Moore et al., 2019). Furthermore, increasing MYI export through these channels has implications for ships operating downstream along the Northwest Passage (Howell et al., 2022; Pizzolato et al., 2014) and as far south as Newfoundland (Barber et al., 2018). Ice export through these channels is limited by the seasonal formation of ice arches (also known as ice bridges or barriers; Hibler et al., 2006; Kirillov et al., 2021; Melling, 2002) that impede ice motion, yet as the Arctic warms these arches are forming for shorter periods and occasionally not forming at all, allowing increased ice export (Howell et al., 2023; Howell & Brady, 2019; Moore, Howell, Brady, et al., 2021). Annual ice export into Nares Strait increased from 33,000 km² between 1996 and 2002 (Kwok, 2005) to 87,000 km² between 2019 and 2021 (Moore, Howell, Brady, et al., 2021) and more recently 95,000 km² between 2017 and 2021 (Howell et al., 2023). Meanwhile, annual ice export into the QEI increased from 8,000 km² between 1997 and 2002 (Kwok, 2006) to 25,000 km² between 1997 and 2018 (Howell & Brady, 2019), with a recent peak of 120,000 km² in 2020 (Howell et al., 2023). Assuming an MYI proportion of 50% in Nares Strait and 100% in the QEI, Babb et al. (2022) used the average total ice export of Howell and Brady (2019) and Moore, Howell, Brady, et al. (2021) to estimate an annual average MYI export of 68,500 km² through these channels. However, Howell et al. (2023) showed that between 2017 and 2021 an average of 113,200 km² of MYI was exported annually through these channels, which far exceeds the estimates of Babb et al. (2022) and is 29% of the estimated annual average MYI export through Fram Strait between 2002 and 2020 (Wang et al., 2022). Overall, MYI export into Nares Strait and the QEI is increasing in magnitude and playing a greater role in the overall MYI budget of the Arctic Ocean.

2.2. MYI Melt

Traditionally, very little MYI was thought to completely melt within the Arctic Ocean (Kwok & Cunningham, 2010) as lateral melt of MYI floes was assumed to be negligible when examining annual records of MYI area (Kwok, 2004a). However, Kwok and Cunningham (2010) found that export alone could not satisfy the dramatic reduction of MYI area in the early 2000s, highlighting the increasing contribution of melt. Although MYI can melt in any area of the Arctic Ocean, there has been a focus on MYI melt within the Beaufort Sea because of its

broader role of retaining MYI within the Beaufort Gyre (Babb et al., 2022; Kwok & Cunningham, 2010). Between 1981 and 2005, 93% of MYI passing through the Beaufort Sea survived through the melt season, facilitating the redistribution of MYI via the Gyre and maintaining a relatively high MYI area in the Arctic Ocean (Maslanik et al., 2011). However, an accelerated ice-albedo feedback increased ice melt in the Beaufort Sea through the 2000s (i.e., Perovich et al., 2008), which led to reductions in MYI thickness (Krishfield et al., 2014; Mahoney et al., 2019) and increased MYI loss (Babb et al., 2022; Kwok & Cunningham, 2010). As a result, between 2006 and 2010 the survival rate of MYI passing through the Beaufort Sea declined to 73% (Maslanik et al., 2011), with approximately one-third of the pan-Arctic MYI loss between 2005 and 2008 being lost to melt in the Beaufort Sea (Kwok & Cunningham, 2010). Using a regional MYI budget, Babb et al. (2022) found that MYI melt in the Beaufort Sea quadrupled between 1997 and 2021, interrupting MYI transport through the Beaufort Gyre and precluding MYI from being advected onwards to other marginal seas. In particular, MYI melt in the Beaufort Sea peaked at 385,000 km² in 2018, which is similar to the estimated magnitude of MYI export through Fram Strait (Babb et al., 2022; Wang et al., 2022).

2.3. MYI Replenishment

As the sole source of MYI, annual replenishment of MYI from FYI that survives the melt season is a critical yet understudied term in the MYI budget. The first estimates of MYI replenishment were presented by Kwok (2004a), who constructed annual cycles of MYI area in the Arctic Ocean by taking the MYI area determined by QuickSCAT on January 1 and then adjusting the area by the record of MYI export through Fram Strait. MYI replenishment was then calculated as the difference between the estimated MYI area during the September minimum (projected forwards from 1 January) and the estimated MYI area in October (projected backward from 1 January). Using this method, replenishment averaged 1.1×10^6 km² from 2000 to 2002 (Kwok, 2004a), though there was subsequently near-zero replenishment in 2005 (Kwok, 2007) and 2007 (Kwok et al., 2009).

Kwok (2007) found that ~63% of the variance in MYI replenishment from 2000 to 2006 was explained by a combination of melting-degree-day (MDD) anomalies during summer and freezing-degree-day (FDD) anomalies during the preceding winter. Generally, warmer temperatures during summer increase ice melt and reduce the likelihood of FYI surviving through summer and replenishing MYI, while colder temperatures during the preceding winter create thicker FYI that is more likely to persist through the melt season and replenish MYI. The importance of ice growth during the preceding winter reflects the negative conductive feedback; thin ice grows faster thermodynamically than existing thick ice, and thereby stabilizes the ice pack (Bitz & Roe, 2004; Notz, 2009). However, this feedback has weakened since 2012 due to the occurrence of warmer winters limiting thermodynamic ice growth (Stroeve et al., 2018), particularly in 2015 when an anomalously warm winter reduced FYI volume by 13% at the end of winter and was proposed to have limited MYI replenishment (Ricker et al., 2017). Ultimately, reduced FYI growth during winter not only encourages lower summer sea ice extents, but also limits MYI replenishment and therefore amplifies annual sea ice loss.

3. Data and Methods

3.1. Ice Age Data Set

The basis for this analysis is the EASE-Grid Sea Ice Age data set from the National Snow and Ice Data Center (NSIDC; Version 4—Tschudi et al., 2019a; updated 2021). The data set provides weekly fields of ice age at 12.5 km resolution across the Arctic Ocean since 1984 and has previously been employed to highlight MYI loss (e.g., Meier et al., 2021; Stroeve & Notz, 2018), and validate other remotely sensed ice-type products (Ye et al., 2023) and modeled MYI coverage (Jahn et al., 2012; Regan et al., 2023). The data set estimates ice age by Lagrangian parcel-tracking through the NSIDC's Polar Pathfinder Sea Ice Motion Data Set (Version 4—Tschudi et al., 2019b; updated 2021) and determining how long a parcel persists. Parcels age by 1-year after the week of the September sea ice minimum so long as the concentration of the grid cell they are in remains above 15%. A similar method was used by Rigor and Wallace (2004) to estimate ice age from gridded ice motion fields derived from buoy tracks, though Nghiem et al. (2006) found that insufficient coverage of buoys at certain times introduced uncertainties in the ice age model. The Ice Age product overcomes this by using an ice drift product that integrates buoy tracks with daily fields of ice motion derived from spaceborne passive microwave radiometers, providing a continuous record of ice motion necessary to track parcels for years.

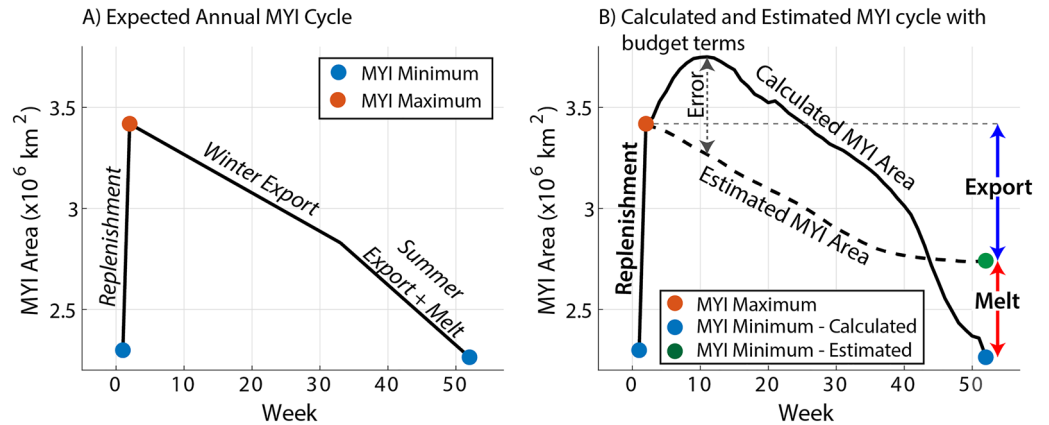


Figure 1. The expected (a), and calculated and estimated (b), annual cycles of multiyear sea ice (MYI) area in the Arctic Ocean, in weeks after the September minimum. Terms of the presented MYI budget are bolded in (b).

The passive microwave record and therefore the ice motion record began in October 1978, yet the Ice Age product requires time to spin up and develop an ice age distribution (up to 5 years); hence it has typically only been available since 1984. However, following the September sea ice minimum of 1979, MYI can be distinguished from FYI, hence our analysis of MYI begins in September 1979 using data available from Meier and Stewart (2023), but ice age distributions are only available since 1984.

One limitation of the Ice Age product is that each grid cell is assigned the age of the oldest parcel within it at that time, meaning that there is no partial MYI concentration like in ice charts (i.e., Babb et al., 2022) or other remotely sensed ice type products (i.e., Comiso, 2012; Kwok, 2004a). As a result, there is an inherent overestimation of MYI area within the data set (Korosov et al., 2018; Tschudi et al., 2016), an error that grows during fall freeze-up when grid cells with low MYI concentrations ($\geq 15\%$) freeze-up completely with new ice but continue to be identified as MYI. Korosov et al. (2018) suggest that this overestimation is greater in the marginal ice zone than the central Arctic because there is a greater mixture of MYI and FYI around the periphery of the ice pack. Additionally, the ice age product is subject to the uncertainty in the ice drift product, which is known to be greater during summer than winter (Sumata et al., 2014), and errors may accrue along the coast due to the way that the tracking system accounts for divergence and convergence from the shore. In particular, offshore winds result in the formation of young ice along the coast, but because the tracker does not compress the ice during onshore winds these areas of young ice may persist and accumulate. This is a particular issue north of Ellesmere Island where areas of young ice are occasionally present in an area that is known to contain the oldest sea ice (Figure 2). Despite these limitations, the Ice Age product has the critical advantage of being available year-round, whereas other remotely sensed ice-type products are confined to the ice growth season because once the ice/snow surface begins to melt, distinguishing ice types becomes more uncertain.

3.2. MYI Budget

To examine the MYI budget of the Arctic Ocean we must define the boundaries, calculate the weekly time series of MYI area within the region (Figure 1), and calculate MYI export across the boundaries. Following Kwok (2004a), the Arctic Ocean was defined by boundaries across Fram Strait, the channels between Svalbard, Franz Josef Land and Severnaya Zemlya, the Bering Strait, the western edge of the CAA and the northern entrance to Nares Strait (Figure 2). MYI area in the Arctic Ocean was calculated by summing the weekly mean sea ice area in pixels identified as MYI within the weekly ice age data set. Sea ice area was calculated from the NSIDC daily passive microwave sea ice concentration data set (Cavalieri et al., 1996; updated 2022). MYI area is characterized by a well-defined annual cycle from a maximum following replenishment to the minimum during September with the decrease in MYI area being the result of export during winter and the combination of export and melt during summer (Figure 1a; Figure S1 in Supporting Information S1).

Critical to the annual cycle and definition of MYI is that MYI is only created by replenishment from FYI that survives through the minimum. Replenishment is calculated as the area of second-year ice (MYI2) during the

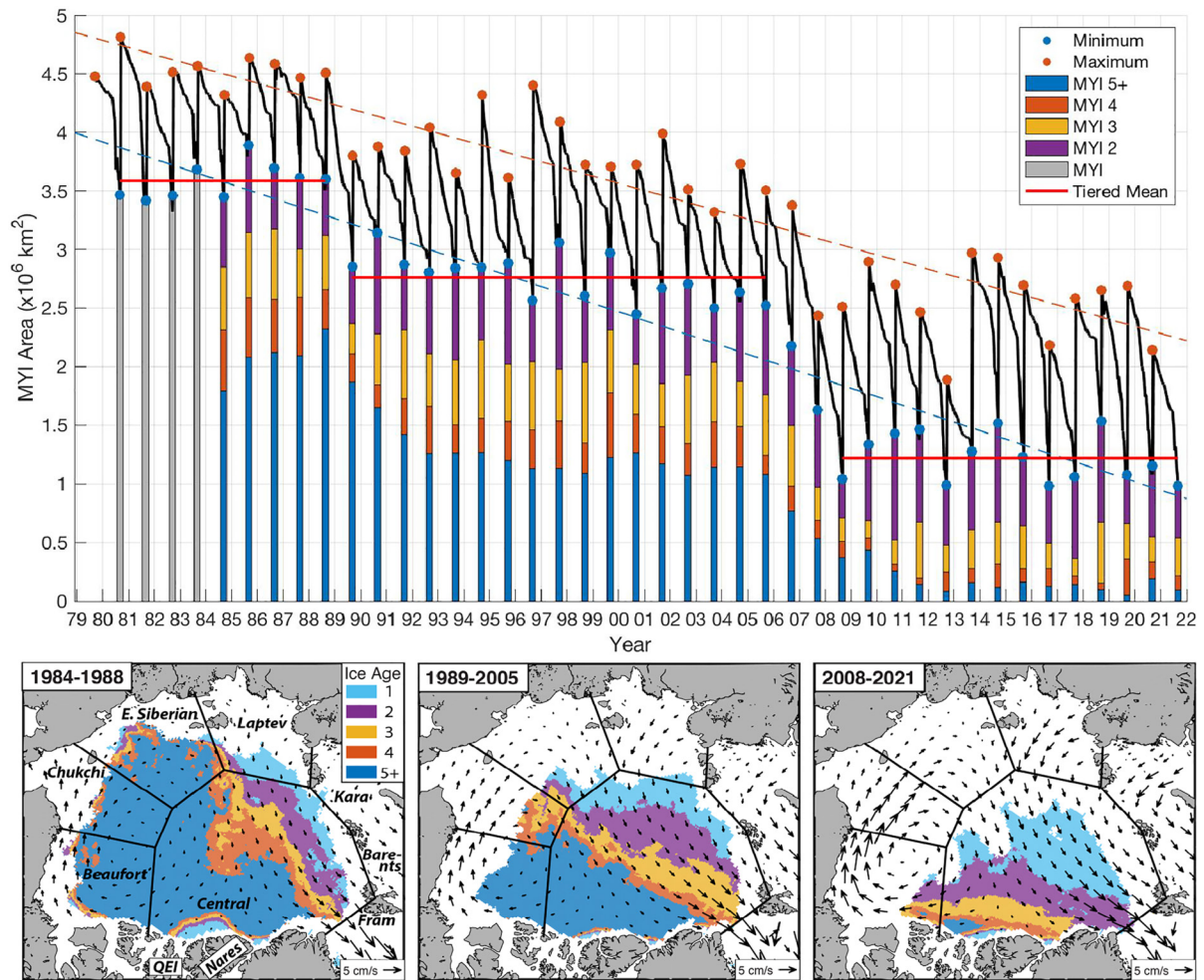


Figure 2. Top: Time series of the weekly multiyear sea ice (MYI) area in the Arctic Ocean beginning the week after the minimum of 1979 and running to the minimum of 2021. The MYI age distribution during the September minimum is presented by colored bars for 1984–2021. Dots denote the MYI area during the minimum and maximum, with associated trend lines shown by dashed lines. The mean MYI minimum during the three periods are overlaid. Bottom: Maps of the median ice age during the minima of each period. The mean annual fields of ice drift are overlaid, and the regional boundaries are also presented.

week after the minimum (Figure 1a). However, the time series of MYI area calculated from the Ice Age data set shows an erroneous increase in MYI area after replenishment, which is the result of concentration increasing within pixels containing at least some portion of MYI during freeze-up. To account for this error, we use a method similar to Kwok (2004a) and create an estimated annual record of MYI area by accounting for MYI export (Figure 1b). We use the maximum and minimum MYI area to bookend the annual record and then account for MYI export across all of the Arctic Oceans boundaries to create a time series of estimated MYI area (dashed line Figure 1b). At the time of the September minimum, we sum the net export for the ice season (blue line Figure 1b) and determine MYI melt as the difference between the estimated MYI area, which is based solely on export, and the calculated MYI area, which reflects MYI lost to export and melt (red line Figure 1b). Because MYI area is inherently overestimated within the Ice Age data set, MYI export and the MYI minimum are overestimated, meaning that MYI melt and MYI replenishment are underestimated. To constrain this error, we calculate the difference between the peak in the calculated MYI area and the estimated MYI area at that time (Figure 1b; Figure S1 in Supporting Information S1). On average 503,000 km² or 15% of the MYI area is erroneously created during freeze-up, most of which is expected to accrue in the marginal seas (Korosov et al., 2018) and therefore have limited effect on our estimates of MYI export through Fram Strait. However, as MYI area has declined this error has increased at a rate of 1.6% per decade. We ascribe this trend to the fact that declining MYI area is not only characterized by a reduction in MYI extent but also a reduction of sea ice concentration within MYI pixels at the end of summer, which agrees with results from Comiso (2012) and leaves a greater area for FYI to form

in MYI pixels. As an example, the maximum error occurred in autumn 2012 (31%; 2013 ice season Figure S1 in Supporting Information S1), following a near-record MYI area minimum during which the MYI pack was dispersed across an area of low sea ice concentrations, leaving a large area within the MYI pack for FYI to form.

An additional source of error in determining MYI area stems from the convergence/divergence of the MYI pack and specifically how this is handled in the Ice Age data set. Theoretically, divergence has no impact on MYI area (area is conserved), whereas convergence leads to deformation which reduces MYI area but conserves MYI volume. Previous work on the annual MYI cycle has assumed that MYI does not deform (Kwok, 2004b), or has acknowledged that it may deform but does not consider deformation as a sink of MYI area (Kwok & Cunningham, 2010). Regan et al. (2023) calculated MYI deformation as convergence of modeled ice motion fields, yet they assumed that FYI was preferentially deformed and the MYI deformation only occurred once all FYI had been deformed. Mimicking this with ice motion fields and the Ice Age data set would introduce significant uncertainty and require additional tracking of each parcel of MYI to determine the actual MYI concentration and cumulative convergence over time. Given this uncertainty in quantifying MYI deformation, we do not account for this term within the MYI budget which may in turn lead to an overestimate of MYI melt.

Ice flux (F) across the boundaries of the Arctic Ocean is calculated at regular intervals using the following equation,

$$F = c u \Delta x \quad (1)$$

where, c is the sea ice concentration, u is the ice velocity component normal to the gate and Δx is the interval. For large channels like Fram Strait, and channels into the Kara and Barents Seas, F was calculated weekly using fields of sea ice drift and concentration from the NSIDC data sets, and used to calculate MYI flux by summing points along the flux gate identified as MYI by the Ice Age data set. Negative fluxes represent MYI export from the Arctic Ocean, while positive fluxes represent MYI import.

For the narrower channels, such as Nares Strait and the QEI, passive microwave products are too coarse, so we rely on previously published values of ice flux that utilize higher-resolution ice drift data. Total ice export into Nares Strait was determined from 1998 to 2009 by Kwok et al. (2010), while Howell et al. (2023) determined total and MYI flux into Nares Strait from 2017 to 2021. To estimate MYI flux prior to 2017 we first estimate total ice flux using the relationship that Kwok et al. (2010) found between the duration of the period when ice drift was unobstructed by ice arches and total ice export. This relationship is approximated to be $F = 285.74 \times \text{duration} - 19,577$, where duration is the number of days during each ice season (September minimum to September minimum) when the arch was not in place. To determine duration, we use the timing of ice arch formation and collapse presented by Vincent (2019) for 1979–2019, while for 2020 and 2021, we use the dates of formation presented by Kirillov et al. (2021) and estimate the date of breakup from daily MODIS imagery. The record of total ice flux into Nares Strait is presented in Figure S2 in Supporting Information S1. Finally, we estimate MYI flux from total ice flux by assuming an MYI proportion of 88%, which is based on the data presented by Howell et al. (2023).

Total ice export into the QEI has been quantified for the period from 1997 to 2002 (Kwok, 2006), 1997–2018 (Howell & Brady, 2019), and more recently 2017–2021 (Howell et al., 2023). MYI flux was also determined during the latter period and revealed that MYI comprises 85% of the total ice flux into the QEI. To build a record of MYI flux into the QEI, we use the values of total ice export from Howell and Brady (2019) for the period 1997–2016, and the average export of 8,000 km² from Kwok (2006) for the period 1979–1996, then scale them by 85%.

MYI flux through Amundsen Gulf and M'Clure Strait are not considered in this budget. Amundsen Gulf is predominantly covered by seasonal ice and is therefore neither a source or sink of MYI (Babb et al., 2022). M'Clure Strait contains a mix of seasonal and MYI, but recent observations show that the oscillation between export and import averages out to a net seasonal ice flux of only 2 km² (Howell et al., 2023).

Collectively, the terms of MYI export, melt, and replenishment dictate the annual MYI budget (Figure 1b). The budget is summed for the annual ice season, which begins with replenishment after the minimum and runs to the following minimum, providing a net change in MYI area for each year.

Regional boundaries as defined by the NSIDC MASIE (Multisensor Analyzed Sea Ice Extent) mask (Figure 2) were used to quantify MYI transport between regions within the Arctic Ocean and to breakdown replenishment by region.

3.3. Ancillary Data

Monthly mean fields of 2 m air temperature (T) were retrieved from the ERA-5 reanalysis (Hersbach et al., 2020) and used to calculate the cumulative FDD ($T < -1.8^{\circ}\text{C}$) from October to May, and MDD ($T > 0^{\circ}\text{C}$) from June to September. MDD was tested for a correlation with MYI melt, while following Kwok (2007), the combination of FDD and MDD were tested for correlation with MYI replenishment.

4. Results and Discussion

4.1. MYI Area

Over the 43-year study period, the annual MYI minimum and maximum areas declined significantly ($p < 0.05$) at $-72,500 \text{ km}^2 \text{ year}^{-1}$ and $-61,000 \text{ km}^2 \text{ year}^{-1}$, respectively (Figure 2a). The minimum MYI area declined at a higher rate than the decline in minimum total sea ice area within the Arctic Ocean ($-59,000 \text{ km}^2 \text{ year}^{-1}$), indicating MYI is being lost at a greater rate than FYI. However, the reduction in the minimum MYI area has not occurred linearly, nor in eight to 9 year cycles as proposed by Comiso (2012), but rather through two stepwise reductions that interrupt three periods of relative stability in MYI area. The first stepwise reduction occurred between September 1988 and 1989, and coincides with the “flushing” of MYI through Fram Strait (Pfirman et al., 2004). The second stepwise reduction occurred between September 2005 and 2008, which is known to be a period of increased MYI loss (Kwok, 2009) that is thought to have been conditioned by the first reduction in 1989 (Lindsay et al., 2009) and corresponds to a shift toward thinner ice across the Arctic Ocean (Sumata et al., 2023). The average minimum MYI area during these periods fell from $3.56 \pm 0.14 \times 10^6 \text{ km}^2$ between 1980 and 1988, to $2.7 \pm 0.23 \times 10^6 \text{ km}^2$ between 1989 and 2005, and finally $1.2 \pm 0.20 \times 10^6 \text{ km}^2$ between 2008 and 2021. The minima during the three periods have statistically different means ($p < 0.01$).

The reduction in MYI area between the three periods was accompanied by a change in the spatial distribution of MYI in the Arctic Ocean with a retreat of the MYI edge toward the northern coast of Greenland and the CAA (Figure 2b). From 1980 to 1988, MYI covered much of the Arctic Ocean, with older ice types being advected through the Beaufort Gyre and remnant FYI being confined to the perimeter of the summer ice edge. From 1989 to 2005, a wide band of the oldest MYI was present along the coasts of the CAA and Greenland, stretching from the Beaufort Sea to Fram Strait, while FYI remained intact in the central Arctic and spanned across the eastern face of the ice pack. Following the collapse of MYI between 2006 and 2008, MYI coverage between 2008 and 2021 was dramatically altered compared to the previous periods. The oldest MYI types were typically only present immediately along the CAA with a portion extending into the Beaufort Sea and none of the oldest ice reaching Fram Strait. Furthermore, the reduction in MYI area coincides with an increase in ice drift speeds during each period (Figure 2b) as a younger ice pack is mechanically weaker and therefore more mobile (Kwok et al., 2013; Rampal et al., 2009).

The reduction in MYI area has been compounded by a dramatic loss of older MYI types (Figure 2). During the annual minimum, the area of MYI 3 years and older decreased 81% from $3.06 \times 10^6 \text{ km}^2$ in the first period to $0.59 \times 10^6 \text{ km}^2$ in the third period. The reduction is even more dramatic for MYI 5+ years old, which decreased 92% from $2.08 \times 10^6 \text{ km}^2$ in the first period to $0.17 \times 10^6 \text{ km}^2$ in the third period, and is likely even lower given that MYI area is skewed toward older ice types in the Ice Age data set. Over the 43-year study period, there are significant ($p < 0.01$) negative trends in the area of MYI 3 ($-7,800 \text{ km}^2 \text{ year}^{-1}$), 4 ($-9,400 \text{ km}^2 \text{ year}^{-1}$), and 5+ ($-59,000 \text{ km}^2 \text{ year}^{-1}$) years old, but interestingly there is no trend in second-year ice area, which has remained stable around its mean minimum of $0.65 \times 10^6 \text{ km}^2$ but now comprises a greater proportion of the MYI pack.

4.2. MYI Budget

To examine MYI loss during these two stepwise reductions and the equilibrium in MYI area that has existed during the three periods they separate, we now analyze the three terms and net annual balance of the MYI Budget.

4.2.1. MYI Export

On average $709,000 \text{ km}^2$ of MYI was exported from the Arctic Ocean annually over the record (Figure 3). A vast majority ($648,300 \text{ km}^2$; 93%) of the export was through Fram Strait (Figure 3b) while the remaining 7% represents the balance of (a) export into Nares Strait and the QEI and (b) transport (either import or export) across the boundaries to the Barents and Kara Seas.

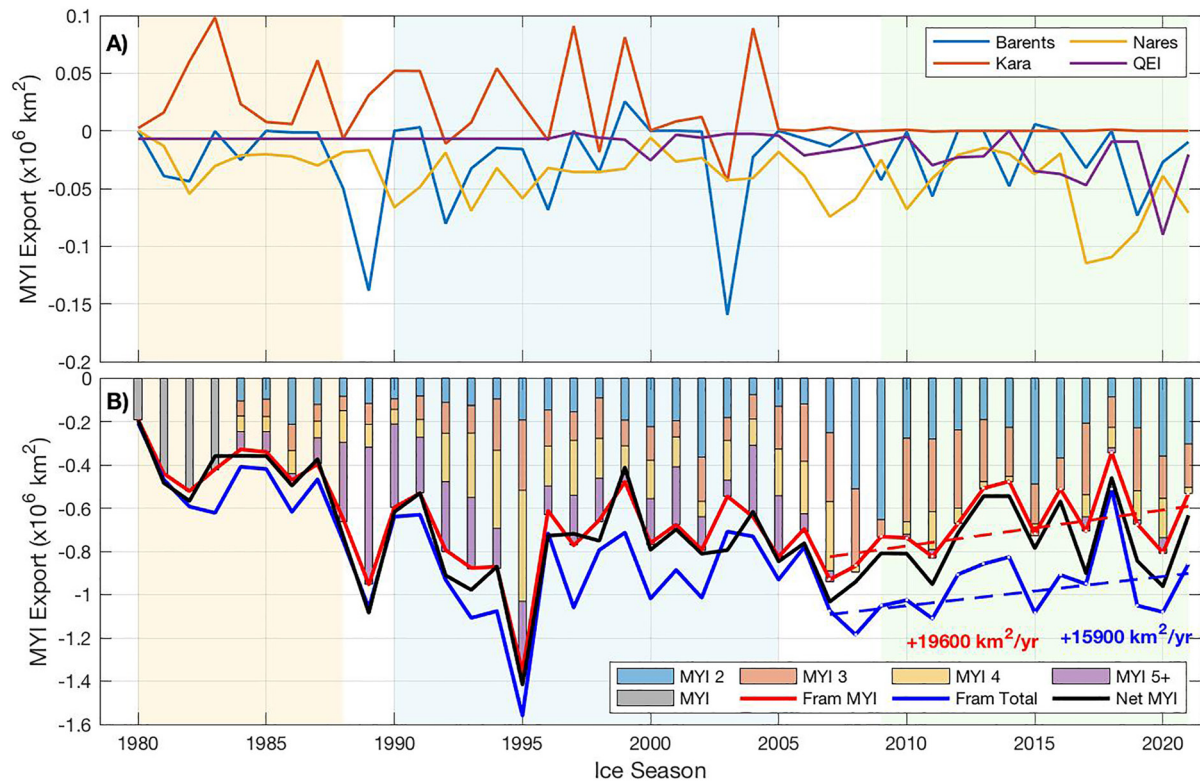


Figure 3. Annual record of multiyear sea ice (MYI) export across the boundaries of the Arctic Ocean from the ice season of 1980–2021. Top: MYI transport into Nares Strait and the QEI, Barents Sea, and Kara Sea. Bottom: MYI and total ice transport through Fram Strait, along with the net MYI export for each year and the MYI age distribution of MYI export through Fram Strait (bars). Positive values indicate import, while negative values indicate export. Significant trends are presented with dashed lines.

MYI export from the Arctic peaked at $1.4 \times 10^6 \text{ km}^2$ in 1995 (Figure 3). This agrees with the observed peak in total ice export through Fram Strait presented by Kwok (2009), which the authors attributed to an increased sea level pressure gradient across the strait that enhanced ice drift speeds. Total MYI export has only surpassed $1 \times 10^6 \text{ km}^2$ two other times, 1989 and 2007, both of which contributed to the two stepwise reductions. In 1989, a record amount of the oldest MYI (MYI 5+; $634,000 \text{ km}^2$) was exported through Fram Strait after it had been flushed out of the Beaufort Gyre by a change in the AO (Figure 3; Pfirman et al., 2004). In 2007, a strong Transpolar Drift Stream increased ice export through Fram Strait (Nghiem et al., 2007), while anomalous ice export into Nares Strait (Kwok et al., 2010) compounded the total MYI export (Figure 3). For comparison, the minimum MYI export through Fram Strait occurred in 2018 ($340,000 \text{ km}^2$) which coincides with an anomalous drop in sea ice volume export (Sumata et al., 2022).

Following the second stepwise reduction from 2006 to 2008, the age distribution of MYI being exported through Fram Strait was much younger, with the proportion of MYI 4+ years declining from 57% of the ice pack prior to 2007 to only 15% after 2007 (Figure 3b). Additionally, since 2007, both MYI and total ice export through Fram Strait declined significantly ($p < 0.05$) with respective rates of $-19,600$ and $-15,900 \text{ km}^2 \text{ year}^{-1}$ (Figure 3b). The discrepancy in these rates has reduced the MYI proportion of the total ice export through Fram Strait from an average of 83% prior to 2007 to 69% since 2007, with the proportion never exceeding 75% since 2007 and reaching a minimum of 56% in 2016. The shift agrees with the transition toward younger thinner ice in Fram Strait identified by Sumata et al. (2023), while the variability in the proportion of MYI highlights the issue with estimating MYI export as a constant proportion of the total ice export (i.e., Babb et al., 2022; Kwok & Cunningham, 2015). Over the full study period, the MYI proportion of the total ice export through Fram Strait has significantly ($p < 0.01$) declined at a rate of -6% per decade. Overall ice export through Fram Strait has shifted to more FYI and younger MYI, a change which is due to younger ice within the Transpolar Drift Stream (Figure 2; Comiso, 2012; Haas et al., 2008; Krumpen et al., 2019), and has undoubtedly contributed to the long-term reduction in sea ice volume export through Fram Strait (Kwok, 2009; Sumata et al., 2022).

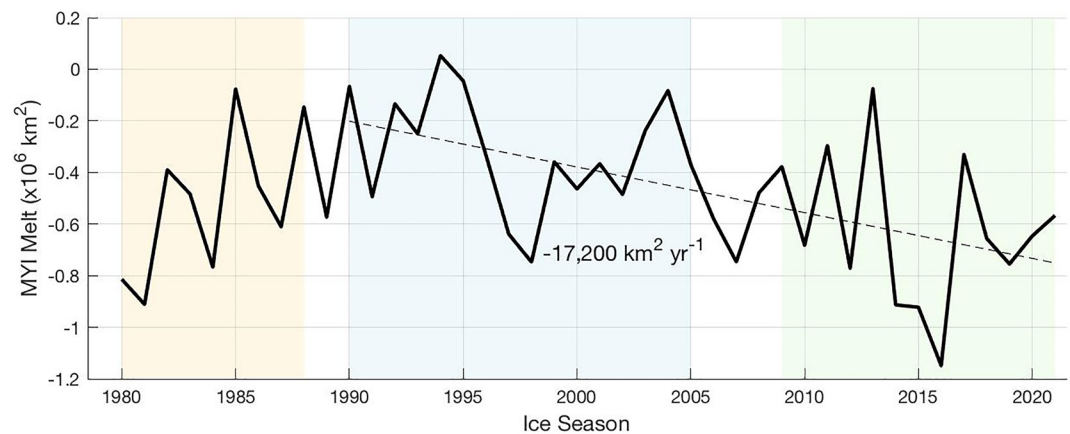


Figure 4. Annual area of multiyear sea ice (MYI) melt for the Arctic Ocean. The dashed line shows the negative trend from 1990 to 2021. The significant trend is presented as a dashed line.

Decreasing MYI export through Fram Strait has been partially offset by increasing MYI export into Nares Strait and the QEI, though the magnitudes of these increases are substantially lower than the trend in Fram Strait (Figure 3a). Historically, a small amount of MYI was imported into the Arctic Ocean from the Kara Sea; however, this source of MYI has been null since 2007 (Figure 3a). MYI export into the Barents Sea peaked at 160,000 km² in 2003, which corresponds to the peak observed by Kwok et al. (2005), but has a long-term mean of only 12,900 km² year⁻¹ with no long-term trend. Following the second stepwise reduction, MYI export into the Barents Sea has been null during half of the years.

Overall, following the second stepwise reduction a significant ($p < 0.05$) negative trend in MYI export through Fram Strait has been slightly offset by increasing MYI export into Nares Strait and the QEI, but overall the net annual MYI export from the Arctic has decreased at a rate of 19,200 km² year⁻¹ (Figure 3b). While on average 93% of the MYI export was through Fram Strait, this proportion declined from 95% prior to 2007 to 87% since 2007, as the consolidation of MYI in the central Arctic and decreases in ice arch duration within Nares Strait and the QEI (Howell & Brady, 2019; Moore, Howell, Brady, et al., 2021) has altered the balance of MYI export.

4.2.2. MYI Melt

Across the Arctic Ocean, an average of 481,000 km² of MYI was lost to melt annually between 1980 and 2021 (Figure 4). MYI melt peaked at 1.15×10^6 km² in 2016 and was near 0 km² in 1994. There is no significant trend over the full 43-year record, though there is a significant ($p < 0.01$) negative trend of $\sim 17,200$ km² year⁻¹ since the first stepwise reduction. Based on the results of Babb et al. (2022), approximately one-third of this increase has occurred in the Beaufort Sea, where MYI melt increased at a rate of 6,000 km² year⁻¹ between 1997 and 2021, causing MYI transport through the Beaufort Gyre to be interrupted. Coincident to the increase in MYI melt has been a significant increase in MDD over the Arctic Ocean of 2 degree-days year⁻¹, that is, 82 degree-days total over the study period (Figure 5). MYI melt and MDD are significantly correlated ($r = 0.38$, $p < 0.01$) with melt increasing by 3,300 km² for every additional degree-day increase in MDD.

4.2.3. MYI Replenishment and Retention

MYI replenishment is the largest term in the MYI budget, averaging 1.11×10^6 km² per year (Figure 6a). However, as the sole source of MYI it must offset export and melt if the MYI budget is to balance annually. Over the study period, MYI replenishment significantly ($p < 0.05$) increased at a rate of +11,000 km² year⁻¹. The peak in MYI replenishment occurred in 1996 (1.8×10^6 km²), yet the next six largest years of replenishment have all occurred since 2005. The minimum replenishment occurred in 1987 (700,000 km²) and may have helped to condition the first stepwise reduction in 1989, while the largest negative anomalies relative to the positive trend occurred during years of record sea ice minima (1998, 2007, and 2012) and coincide with increased melt (Figure 4) during particularly warm years (Figure 5). However, over the study period replenishment and melt from the same year are not correlated, meaning increased MYI melt does not necessarily correspond to increased FYI melt and thereby reduced MYI replenishment. Although replenishment and melt are not correlated for the same summer, replenishment is negatively correlated ($r = 0.46$, $p < 0.01$) with melt during the following summer.

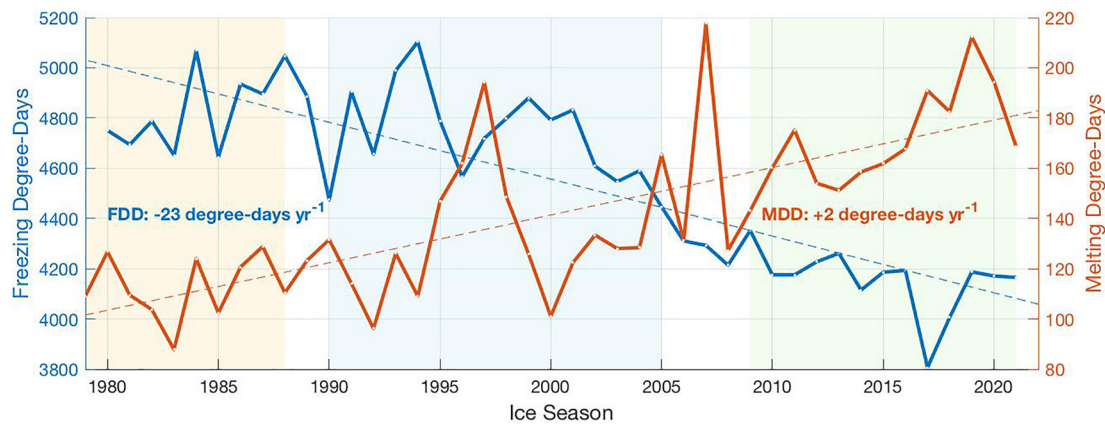


Figure 5. Time series of the spatially averaged freezing-degree-day (FDD) and melting-degree-day (MDD) over the Arctic Ocean from October to May and June to September, respectively. Significant trends are presented by dashed lines.

This relationship is important; increasing replenishment creates a thinner MYI pack during the following melt season, increasing the area of MYI that melts.

Our values of MYI replenishment are significantly higher than those previously presented by Kwok (2004a, 2007) and Kwok et al. (2009). Particularly in 2005 and 2007 when those studies showed near-zero replenishment ($<0.1 \times 10^6 \text{ km}^2$), and we calculated replenishment of $0.93 \times 10^6 \text{ km}^2$ and $0.83 \times 10^6 \text{ km}^2$, respectively. The reason for this discrepancy is the different methods used to calculate replenishment. We calculate the area of second-year ice 1 week after the minimum from the Ice Age data set, which accounts for the reduction in MYI area not just through export but also through melt. The method developed by Kwok (2004a) only accounts for MYI export through Fram Strait and assumes that no MYI is lost to melt. As a result, their method overestimated the MYI area in September, which led to an underestimate of MYI replenishment. Our method also underestimates replenishment as it does not account for surviving FYI within MYI pixels.

Replenishment primarily occurs along the fringe of the summer ice pack where FYI buttresses up against the MYI pack, though a portion does occur within the MYI pack in areas of divergence where FYI has formed (Figure 7). Spatially, replenishment primarily occurs along the eastern side of the ice pack (Figure 7), where FYI that originally formed on the Russian shelves has been advected far enough north to tip the balance of seasonal growth and melt to the point where the ice survives summer. The fact that MYI is replenished on the eastern side and primarily melts in the Beaufort Sea, emphasizes why the two are not correlated, they are spatially disconnected and subject to different forcing during the melt season.

Historically, replenishment was approximately split evenly between the marginal seas and the central Arctic (Figure 6b). That changed during the second stepwise reduction as the summer ice edge retreated north of the regional boundaries and reduced the survival of FYI in the marginal seas. Concurrently, the consolidation of the MYI edge exposed a greater area of the central Arctic to FYI that—protected by colder temperatures at northern latitudes—could persist through the melt season (Figure 7e). As a result, since 2007, MYI replenishment in the Chukchi, East Siberian, and Laptev Seas has decreased by over 50% while MYI replenishment in the central Arctic has doubled. Meanwhile, there has been no change in MYI replenishment in the Beaufort Sea despite an increase in FYI area during winter (Galley et al., 2016). The fact that increasing FYI area during winter has not translated to an increase in MYI replenishment indicates that FYI in the Beaufort Sea is typically not thick enough to survive through the melt season and replenish the MYI pack (i.e., Galley et al., 2013), and further highlights the regional variability and importance of latitude for replenishment. Examining the distribution of replenishment area by latitude during the three periods of MYI stability, we find a clear northward transition over time that coincides with the poleward decrease in air temperatures during the melt season (May–September; Figure 7e). The dramatic reduction in replenishment in the marginal seas has transitioned replenishment from a bimodal distribution with peaks at $\sim 72^\circ\text{N}$ and $\sim 82^\circ\text{N}$ to a unimodal distribution around a peak at $\sim 83^\circ\text{N}$ with very little replenishment occurring south of 75°N since 2008.

Warming between the three periods is also evident, with an increase of $\sim 2^\circ\text{C}$ at 70°N and $\sim 0.5^\circ\text{C}$ at the pole (Figure 7e). Significant ($p < 0.05$) trends toward fewer FDD ($-23 \text{ degree-days year}^{-1}$) and more MDD ($+2$

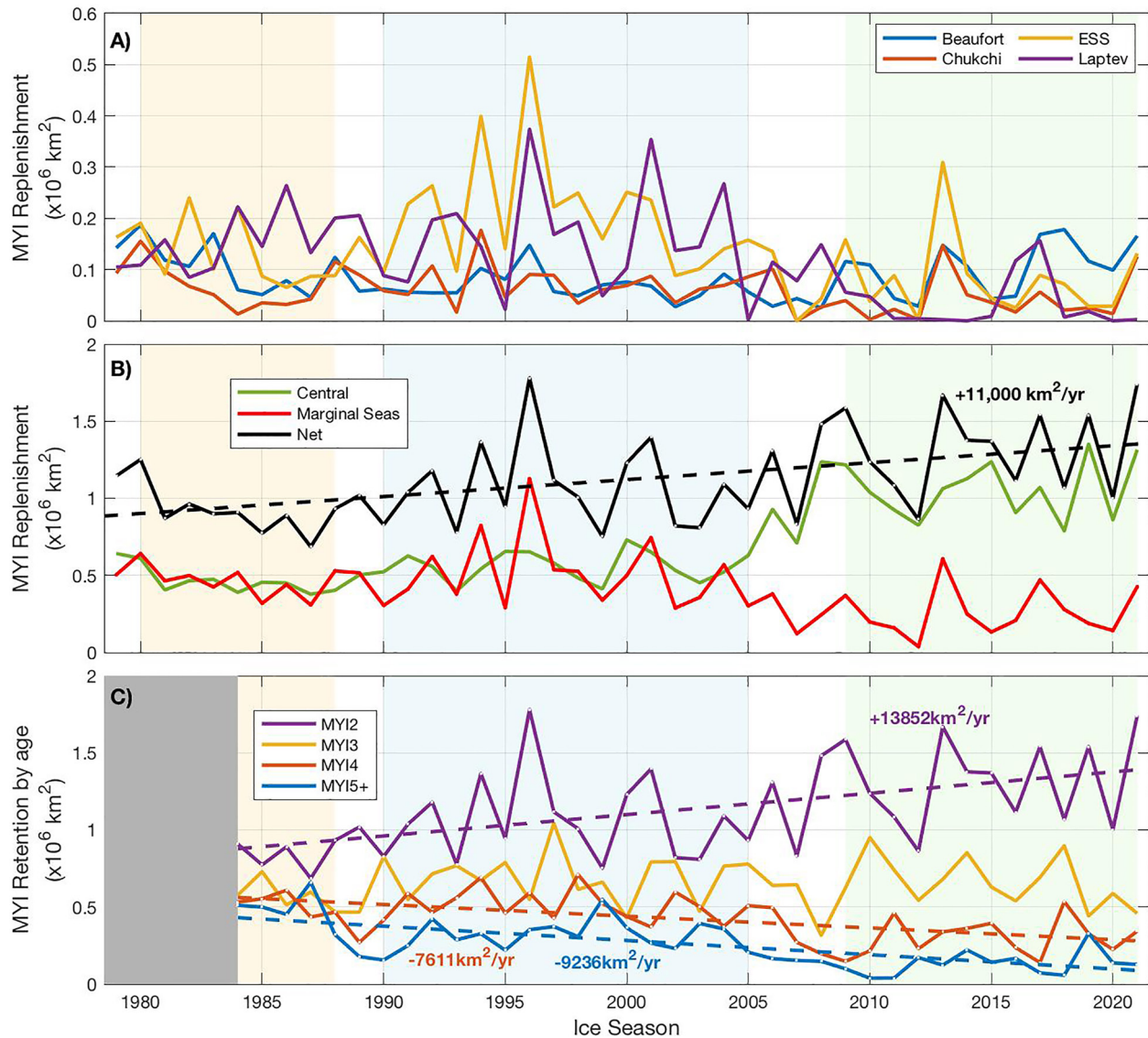


Figure 6. Annual area of multiyear sea ice (MYI) replenishment for (a) each of the marginal seas and (b) the central Arctic and sum of the marginal seas for the total MYI replenishment. (c) MYI retention by age. Note that retention of MYI 2, 3, and 4 are calculated as their area during the week after the minimum, while MYI5+ is calculated as the change in MYI5+ area from their minimum to the week after, representing the increase in area of MYI 5+ and therefore the retention of that age of ice. Significant trends are presented with dashed lines.

degree-days year⁻¹; Figure 5) would intuitively reduce MYI replenishment as there is less FYI growth during winter and more FYI melt during summer. However, we find a clear increase in MYI replenishment that shows no relationship with pan-Arctic MDD and surprisingly a significant inverse relationship with pan-Arctic FDD ($r = -0.45$, $p < 0.01$) that indicates other factors must be driving the observed increase in replenishment. Based on the regional changes in MYI replenishment, it is clear that the increase has primarily been driven by the northward migration of FYI into the central Arctic where it is subject to cooler temperatures and less incident solar radiation facilitating less melt. To support this, we find that the area of both FYI and MYI at the end of winter (the last week of April) are significantly ($p < 0.01$) correlated with MYI replenishment. FYI area has a positive relationship ($r = 0.61$) while MYI area has a negative relationship ($r = -0.61$) implying that more FYI and less MYI at the start of the melt season leads to more MYI replenishment. This highlights a negative feedback in the Arctic system that stabilizes the MYI area by compensating for MYI loss through increased MYI replenishment. However, this MYI feedback requires that FYI grow thick enough during winter to survive the melt season, which is part of the negative conductive feedback (Bitz & Roe, 2004). There is already evidence that the current

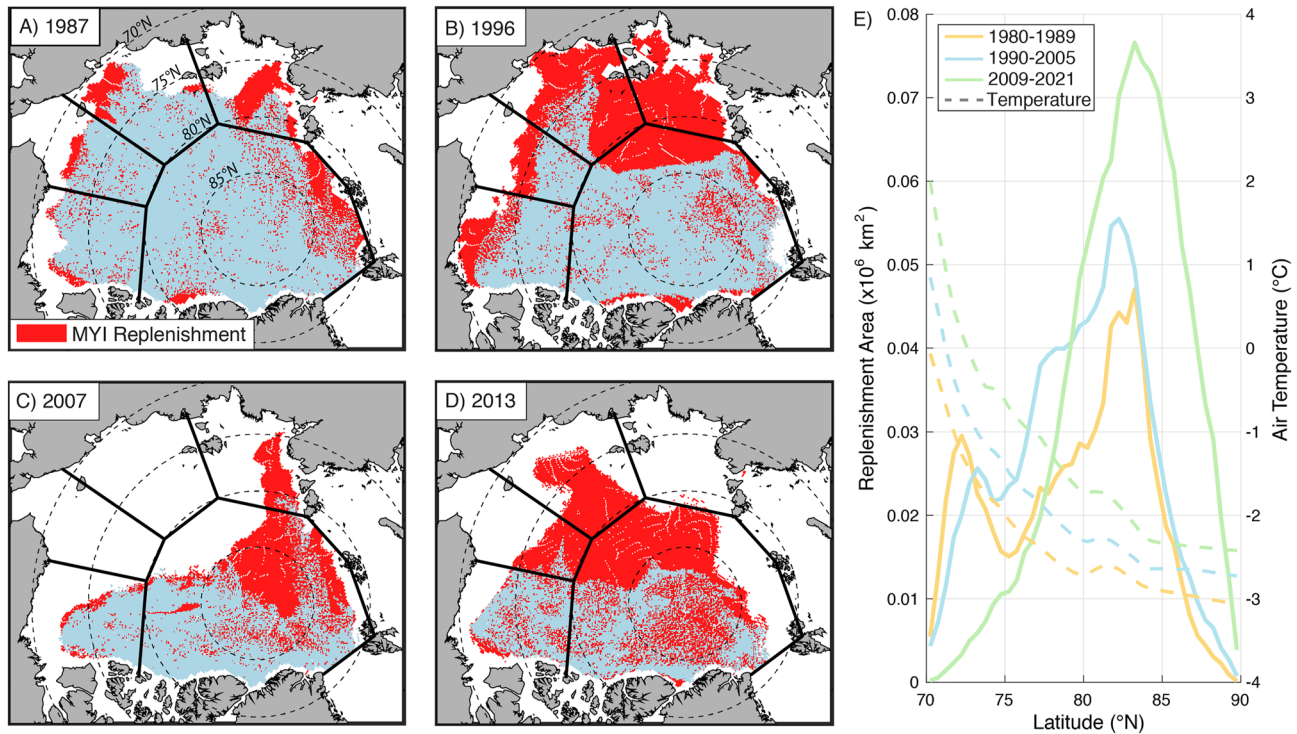


Figure 7. Areas of multiyear sea ice (MYI) replenishment during (a) 1987, (b) 1996, (c) 2007, and (d) 2013. Areas of MYI replenishment are presented in red, while the rest of the ice pack is presented in light blue. Regional boundaries are overlaid in black. (e) Latitudinal distributions of replenishment area (solid lines) and mean air temperature during the melt season (May–September; dashed lines) for the three stable periods of MYI. Note that latitudinal distributions are based solely on data within the boundaries of the Arctic Ocean.

level of warming has weakened the negative conductive feedback (Ricker et al., 2021; Stroeve et al., 2018) and projections that it will eventually be overwhelmed by warming (Petty et al., 2018). Yet in the near term, the MYI feedback may continue to provide some stability to the MYI pack.

A limitation to the stability that results from the MYI feedback is that MYI replenishment only reflects the retention of FYI into second-year ice, while MYI of all ages are lost to export and melt. This imbalance highlights an underlying transition in the MYI pack toward younger and therefore thinner MYI that is undercutting the stability that the positive trend in replenishment is facilitating. Hence, the continued retention of sea ice into progressively older and thicker MYI is key to maintaining the MYI pack. Over the 43-year study period, the retention of second-year ice significantly increased and the retention of MYI 3 years old was fairly stable, while retention of MYI 4 and 5+ years old significantly declined (Figure 6c). The reduced retention of older MYI types is primarily due to the increase in MYI melt in the Beaufort Sea (Babb et al., 2022) which has interrupted MYI transport through the Beaufort Gyre and therefore precludes ice from aging while being retained within the Gyre. As it is now, MYI is only able to age for as long as it can remain in the Central Arctic before it is either siphoned off into the Beaufort Sea, exported into Nares Strait or the QEI, or advected toward Fram Strait.

4.2.4. MYI Budget of the Arctic Ocean

With each of the three MYI terms calculated, we now close the annual MYI budget of the Arctic Ocean for the ice seasons from 1980 to 2021 and determine the net balance for each year (Figure 8a). The net balance shows very close agreement with the change in MYI area calculated from one minimum to the next, indicating our budget captures the vast majority of the changes in MYI area within the Arctic Ocean (Figure 8b). The average annual terms of the MYI budget are; (a) export: $-709,000 \text{ km}^2$, (b) melt: $-463,000 \text{ km}^2$, and (c) replenishment: $1,106,000 \text{ km}^2$, for an average annual loss of $65,000 \text{ km}^2 \text{ year}^{-1}$ over the 43 years study period. However, there is considerable variability between years of MYI loss and MYI gain. The greatest MYI loss occurred in 1989 ($-719,000 \text{ km}^2$), driving the first stepwise reduction in MYI area. The record loss in 1989 was the result of positive anomalies in export (+56%; $+387,140 \text{ km}^2$) and melt (+19%; $+92,450 \text{ km}^2$) coupled with a

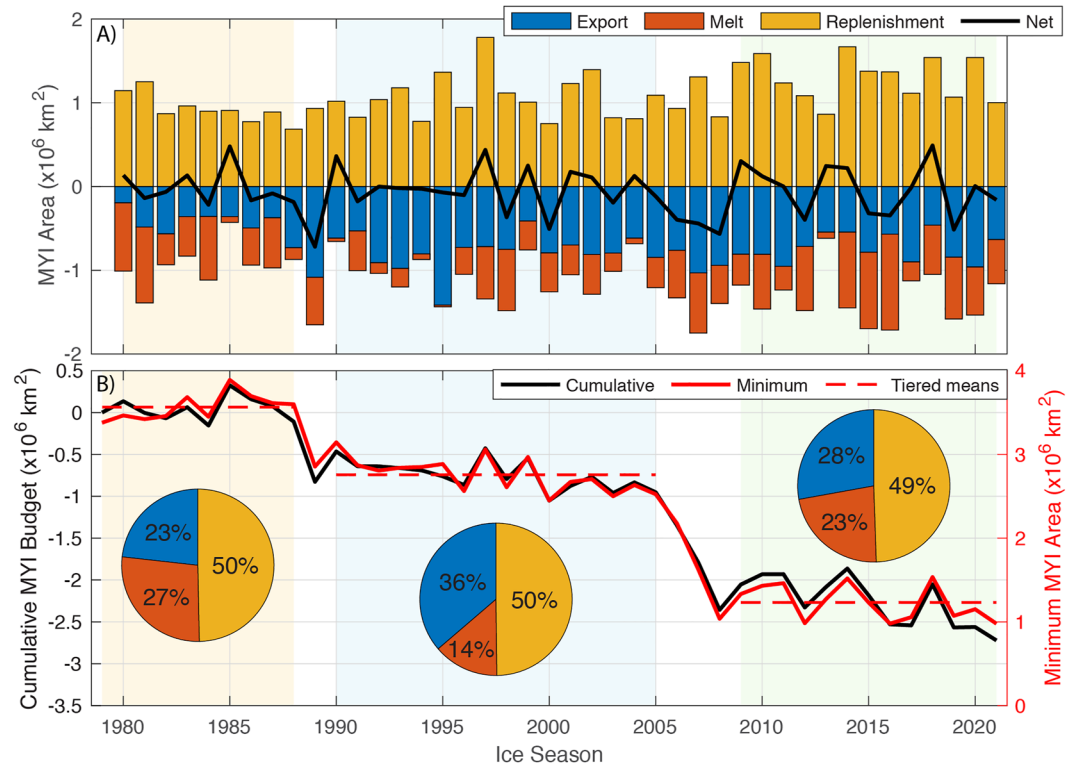


Figure 8. Top: Stacked bar plots of the annual multiyear sea ice (MYI) budget with the net overall results presented in black. Bottom: Time series of the cumulative annual result of the MYI budget (blue) and the MYI area minimum (red). Pie charts of the average contribution of each term to the overall budget are presented for each of the three periods of MYI stability are highlighted by shading.

negative anomaly in replenishment (-16% ; $-174,590 \text{ km}^2$). Conversely, the highest MYI gain occurred in 2018 ($490,000 \text{ km}^2$), due to a negative anomaly in export (-43% ; $-295,870 \text{ km}^2$) and positive anomaly in replenishment ($+39\%$; $+434,200 \text{ km}^2$), and despite a positive anomaly in melt ($+36\%$; $+175,180 \text{ km}^2$). Contrasting between years of MYI loss and gain against the mean magnitude of each term, reveals that a net loss corresponds to greater export ($+57,000 \text{ km}^2$) and melt ($+26,000 \text{ km}^2$) and much less replenishment ($-95,000 \text{ km}^2$), while a net gain corresponds to reduced export ($-93,000 \text{ km}^2$) and melt ($-42,000 \text{ km}^2$) and much more replenishment ($+155,000 \text{ km}^2$). While all three terms contribute to the direction of the net balance, replenishment has the greatest magnitude and even exceeds the combined anomaly of export and melt during years with a net gain or net loss; hence replenishment has the greatest influence on the overall net MYI balance.

Beyond the MYI balance of an individual year, it is important to look at the balance over a few years as individual years of MYI loss or gain can often be offset by a contrasting swing in subsequent years that can either stabilize the MYI pack or dramatically (and permanently) change it. For example, between 1995 and 2001 the MYI budget oscillated between large losses and gains, with the peak export (1995) and replenishment terms (1996) terms occurring during this period, but overall they offset each other and the MYI area remained relatively stable through this time (Figure 8). Similarly, the loss of MYI in 2012, which was primarily due to anomalously high melt ($+60\%$; $290,870 \text{ km}^2$), was immediately offset by MYI gains in 2013 and 2014. This recovery was the result of cooler temperatures and a consolidated ice pack through the 2013 melt season (Kwok, 2015; Tilling et al., 2015) which reduced melt in 2013 (-84% ; $-405,550 \text{ km}^2$) and led to record replenishment in 2014 ($+51\%$; $+562,690 \text{ km}^2$; occurring during fall 2013). However, losses are not always offset in subsequent years. For example, the second stepwise reduction in MYI area occurred between 2006 and 2008 when approximately $1.4 \times 10^6 \text{ km}^2$ of MYI was lost, which is slightly less than the MYI area loss of $1.54 \times 10^6 \text{ km}^2$ reported by Kwok et al. (2009). Focusing on this period of MYI loss, we find that 2006 was characterized by increased melt ($+21\%$; $+99,000 \text{ km}^2$) and reduced replenishment (-16% ; $-174,850 \text{ km}^2$) with near average export ($+9\%$; $+58,821 \text{ km}^2$). 2007 was characterized by increased export ($+45\%$; $+312,930 \text{ km}^2$) and melt ($+55\%$; $+265,700 \text{ km}^2$), and

actually experienced increased replenishment relative to the long-term mean (+18%; +201,890 km²; opposite to what Kwok et al., 2009 showed). 2008 had the second greatest annual loss of MYI on record and was primarily the result of increased export (+33%; +227,950 km²) and reduced replenishment (−25%; −275,400 km²; from autumn 2007) with near-average melt (0%). Clearly it was not just one term that facilitated the second stepwise reduction in MYI area but rather anomalous export, melt, and replenishment over consecutive years steadily compounding the overall decline and driving a significant change in the MYI pack.

During the three periods of stability in the minimum MYI area, melt and export were in equilibrium with replenishment (Figure 8b). However, the proportion of export and melt changed between periods. During the first period export and melt were similar in magnitude, whereas during the second period export was more than twice as great as melt. During the third period, the two returned to being approximately equal in magnitude, cleanly breaking the budget down between approximately one-quarter melt, one-quarter export, and one-half replenishment. With trends toward declining export and increasing melt, the role of each term in the MYI budget is likely to continue swinging toward MYI melt exceeding MYI export. For reference, MYI melt exceeded MYI export during only nine of the 43 years analyzed here, though five of these have occurred since 2010, highlighting the increasing role of MYI melt in the MYI budget of the Arctic Ocean.

4.3. The Future of MYI

The Arctic is projected to be seasonally ice-free ($<1 \times 10^6$ km²) as soon as the 2030s or 2050s (Kim et al., 2023; Notz & SIMIP Community, 2020), at which point the Arctic Ocean will only be seasonally covered by FYI while a small area of MYI will be confined to the northern regions of CAA and Greenland known as the Last Ice Area. The projected near-complete loss of MYI in the not-too-distant future indicates the MYI budget of the Arctic Ocean will continue to be in a deficit. Based on our results, we can expect that future MYI loss will likely occur through a series of stepwise reductions with periods of relative stability in between. Using the MYI budget, we speculate on the contribution of each term to the future loss of MYI.

First, it is worth noting that any appreciable recovery of MYI is highly unlikely in the foreseeable future as that would require several years of reduced MYI loss (export and melt) coupled with increased replenishment and further retention of MYI into older and thicker MYI. Individual years of recovery do continue to occur (i.e., 2013 and 2018; Figure 8) and maintain the current state of equilibrium, yet a stepwise increase in MYI area would require several consecutive years with a net gain in MYI area and most importantly retention into older MYI that is thicker and therefore more resilient against melt. This has not happened at any point over the satellite era.

Export drove the first stepwise reduction in 1989 and contributed to the second reduction between 2006 and 2008. However, the consolidation of the MYI pack away from the area upstream of Fram Strait has led to a negative trend in MYI export since 2008 that has reduced the overall impact of export on the MYI budget and leads us to suggest that export will not be a main driver of future MYI loss. Instead, we speculate that the future loss of MYI will be driven by the combination of high melt and low replenishment, reinforced over several consecutive years. Given that these two terms are related to ice melt, it is intuitive that a particularly warm summer would increase both FYI and MYI melt, with the former limiting replenishment. Conditioning during the preceding winter is also critical to these terms as a strong Beaufort Gyre would expose more MYI to increased melt rates in the Beaufort Sea (i.e., 2021; Babb et al., 2022; Mallett et al., 2021) while a warm winter would limit FYI growth and therefore replenishment (i.e., 2015; Ricker et al., 2017). Considerable MYI replenishment is already occurring in the Central Arctic (Figure 7), where surface air temperatures in the Arctic are coldest, enabling a long-term positive trend in replenishment. However, with further reductions in September sea ice extent, the area available for FYI to survive and replenish MYI will dwindle, causing the positive trend in replenishment to level off and eventually decline.

MYI area melt is likely to continue increasing in the coming years as air temperatures increase (greater MDD, lower FDD), while a transition of the MYI pack itself toward younger thinner MYI makes it less resilient and more susceptible to melt. The transition to younger ice types is being driven by an imbalance between ice of all ages being lost to export and melt, whereas only the replenishment of second-year ice is increasing in contrast to reduced retention of older MYI ages. As a result, the MYI cover continues to thin (Kacimi & Kwok, 2022; Krishfield et al., 2014; Kwok & Rothrock, 2009; Petty et al., 2023), making it more mobile and facilitating the formation of large polynyas within the Last Ice Area during recent years (Moore, Howell, & Brady, 2021;

Schweiger et al., 2021). As a result, Schweiger et al. (2021) suggest that the remaining MYI pack is proving to be less resilient to warming than previously expected.

Ultimately, we speculate that the future loss of MYI is likely to be driven by gradually increasing melt and reduced replenishment, but conditioned by the transition toward a younger thinner MYI pack. With each reduction, the MYI pack will retreat even further toward the Last Ice Area along the coast of the CAA. Eventually, the Arctic Ocean is projected to become seasonally ice-free, at which time the remaining MYI will be confined to the narrow channels of the CAA, and there will be no replenishment within the Arctic Ocean.

5. Conclusions

The loss of MYI and transition to a predominantly seasonal ice cover in the Arctic Ocean has been one of the greatest changes to take place in the Arctic. Using a 43-year data set on sea ice age, we have examined the loss of MYI area and the relative contribution of melt, export, and replenishment to this loss. Overall, MYI area during the annual September sea ice minimum has significantly declined at a rate of $-72,500 \text{ km}^2 \text{ year}^{-1}$; however, MYI loss has not occurred continuously but rather through two stepwise reductions that separated three prolonged periods of relative stability. During these stable periods, MYI loss through export and melt was wholly offset by replenishment, maintaining equilibrium within the MYI pack. Conversely, during the two stepwise reductions, MYI loss greatly exceeded replenishment, driving a dramatic reduction in MYI area and a concurrent northward contraction of the MYI pack toward the coast of the CAA. The first reduction occurred in 1989 after a change in the AO flushed MYI out of the Beaufort Gyre into the Transpolar Drift Stream and subsequently led to anomalously high MYI export through Fram Strait, with a peak in the export of the oldest MYI types. The second reduction occurred between 2006 and 2008 and was the result of anomalously high melt and export, coupled with anomalously low replenishment. The consolidation of the MYI pack during the second reduction reduced the presence of MYI upstream of Fram Strait, leading to a significant decline in MYI export and transition toward younger ice being exported through Fram Strait. At the same time, MYI export into Nares Strait and the QEI has increased, albeit at a much smaller magnitude; however, MYI export through these pathways is important because it is the oldest MYI that is lost.

While there is no long-term trend in MYI export, MYI melt has significantly increased since 1989 while MYI replenishment has significantly increased over the full 43-year study period. The trend in MYI melt is the result of warming temperatures and a transition to younger and thinner MYI that is less resilient to warmer temperatures and the associated ice-albedo feedback. MYI area melt is found to be correlated with MDD and increases $3,300 \text{ km}^2$ for every additional degree-day above 0°C . The trend in replenishment is not correlated with MDD, even though replenishment should reflect FYI melt, or FDD, which reflects FYI growth during the preceding winter. Instead, we suggest that the increase in replenishment has been driven by the northward contraction of the MYI edge which in turn provides greater space for FYI to survive through the melt season at higher latitudes; highlighting a negative feedback that serves to stabilize the MYI pack. While the increase in replenishment has dampened MYI loss and fostered three periods of stability, there is an underlying transition toward younger MYI as the retention of MYI to older ice types has declined. This is a change dominated by increasing melt in the Beaufort Sea interrupting the transport of MYI through the Beaufort Gyre which precludes the ice from aging as it had historically. Additionally, replenishment is found to be correlated with melt during the following summer, meaning that increased replenishment promotes a younger thinner MYI pack that is more susceptible to melt.

Overall, the MYI pack has been stable around a minimum area of $1.2 \times 10^6 \text{ km}^2$ since 2008. However, this stability has been undercut by the continued transition to younger and thinner MYI, with the recent occurrence of large polynyas within the MYI pack suggesting it is not as resilient as previously expected and may be poised for another stepwise reduction. Eventually, the Arctic is projected to be seasonally ice-free, at which point MYI will be confined to the narrow channels of the CAA. In the meantime, we expect MYI loss to continue to occur episodically rather than continuously. The two previous stepwise changes reduced Arctic MYI area by 0.9 and $1.5 \times 10^6 \text{ km}^2$, meaning that a future reduction of similar magnitude would render the Arctic Ocean essentially MYI free. Based on the budget, we do not expect MYI to recover, and we expect future loss to mainly be driven by the combination of increased melt and reduced replenishment. Both of these mechanisms are promoted by warming trends during summer and conditioned by a combination of MYI transport and FYI growth during the preceding winter. Ultimately, the MYI budget of the Arctic Ocean reflects a balance of several factors that have generally been in equilibrium through much of our 43-year study period. However, occasionally MYI loss has

greatly exceeded replenishment, leading to a dramatic reduction and, within the timescale of this study, unrecoverable change in the MYI pack. While a negative feedback in MYI replenishment has so far dampened MYI loss, continued warming that both increases MYI melt and limits MYI replenishment will eventually lead to the complete loss of MYI and transition to a seasonally ice-free Arctic Ocean.

Data Availability Statement

Sea ice concentration, drift and age data sets are available from the National Snow and Ice Data Center (NASA-Team sea ice concentration—Cavalieri et al., 1996; Polar Pathfinder 25 km Drift v4—Tschudi et al., 2019b; EASE-Grid Sea Ice Age v4—Tschudi et al., 2019a). The early EASE—Grid Sea Ice Age data from 1978 to 1983 is available through Zenodo (Meier & Stewart, 2023). ERA5 reanalysis products (Hersbach et al., 2020) are available from the Climate Data Store through the Copernicus Climate Change Service (2023).

Acknowledgments

Tragically D. Barber passed away in the early stages of writing this paper; he was a giant in Arctic research and will be remembered as such. D. Babb, R. Galley, J. Ehn, and D. Barber would like to acknowledge the financial support from the Natural Sciences and Engineering Research Council of Canada (NSERC). D. Babb and S. Kirillov were supported by the Canada Research Chair (CRC—D. Barber) and Canada Excellence Research Chair (CERC—D. Dahl-Jensen) programs. D. Babb acknowledges additional financial support from the Canadian Meteorological and Oceanographic Society (CMOS). J. Landy acknowledges support from the CIRFA project under Grant 237906 and the INTERAAC project under Grant 328957 from the Research Council of Norway (RCN), and from the Fram Centre program for Sustainable Development of the Arctic Ocean (SUDARCO) under Grant 2551323. J. Stroeve acknowledges support from the Canada 150 Chair Program. W. Meier acknowledges support from the NASA Cryospheric Sciences Program (Grant 80NSSC21K0763). We acknowledge the use of imagery from the NASA Worldview application (<https://worldview.earthdata.nasa.gov/>), part of the NASA Earth Observing System Data and Information System (EOSDIS). Thanks to J.S. Stewart at NSIDC for help with the 1979–1983 ice age data. Thanks to M. Bushuk for helpful conversations during the development of this work. Thanks to the editor and two anonymous reviewers for their insightful comments that helped to improve this paper.

References

Babb, D. G., Galley, R. J., Asplin, M. G., Lukovich, J. V., & Barber, D. G. (2013). Multiyear sea ice export through the Bering Strait during winter 2011–2012. *Journal of Geophysical Research: Oceans*, 118(10), 5489–5503. <https://doi.org/10.1002/jgrc.20383>

Babb, D. G., Galley, R. J., Howell, S. E. L., Landy, J. C., Stroeve, J. C., & Barber, D. G. (2022). Increasing multiyear sea ice loss in the Beaufort Sea: A new export pathway for the diminishing multiyear ice cover of the Arctic Ocean. *Geophysical Research Letters*, 49(9), 1–11. <https://doi.org/10.1029/2021GL097595>

Barber, D. G., Babb, D. G., Ehn, J. K., Chan, W., Matthes, L., Dalman, L. A., et al. (2018). Increasing mobility of high Arctic sea ice increases marine hazards off the east coast of Newfoundland. *Geophysical Research Letters*, 45(5), 2370–2379. <https://doi.org/10.1002/2017GL076587>

Bitz, C. M., & Roe, G. H. (2004). A mechanism for the high rate of sea ice thinning in the Arctic Ocean. *Journal of Climate*, 17(18), 3623–3632. [https://doi.org/10.1175/1520-0442\(2004\)017<3623:AMFTHR>2.0.CO;2](https://doi.org/10.1175/1520-0442(2004)017<3623:AMFTHR>2.0.CO;2)

Bourke, R. H., & Garret, R. P. (1987). Sea ice thickness distribution in the Arctic Ocean. *Cold Regions Science and Technology*, 13(3), 259–280. [https://doi.org/10.1016/0165-232x\(87\)90007-3](https://doi.org/10.1016/0165-232x(87)90007-3)

Boutin, G., Ólason, E., Rampal, P., Regan, H., Lique, C., Talandier, C., et al. (2023). Arctic sea ice mass balance in a new coupled ice-ocean model using a brittle rheology framework. *The Cryosphere*, 17(2), 617–638. <https://doi.org/10.5194/tc-17-617-2023>

Cavalieri, D. J., Parkinson, C. L., Gloersen, P., & Zwally, H. J. (1996). Sea ice concentrations from Nimbus-7 SMMR and DMSP SSM/I-SSMIS passive microwave data [Dataset]. Retrieved from <https://nsidc.org/data/NSIDC-0051/versions/1>

Comiso, J. C. (2012). Large decadal decline of the Arctic multiyear ice cover. *Journal of Climate*, 25(4), 1176–1193. <https://doi.org/10.1175/JCLI-D-11-00113.1>

Constable, A. J., Harper, S., Dawson, J., Holsman, K., Mustonen, T., Piepenburg, D., & Rost, B. (2022). Cross Chapter Paper 6: Polar regions. In H. O. Portner, D. C. Roberts, M. Tignour, E. S. Poloczanska, K. Mintenbeck, A. Alegría, et al. (Eds.), *Climate change 2022: Impacts, adaptation and vulnerability* (pp. 2319–2368). Cambridge University Press. <https://doi.org/10.1017/9781009325844.023>

Copernicus Climate Change Service. (2023). Climate change service [Dataset]. Retrieved from <https://cds.climate.copernicus.eu/cdsapp#!/home>

Galley, R. J., Babb, D. G., Ogi, M., Else, B. G. T., Geifus, N. X., Crabeck, O., et al. (2016). Replacement of multiyear sea ice and changes in the open water season duration in the Beaufort Sea since 2004. *Journal of Geophysical Research: Oceans*, 121, 1–18. <https://doi.org/10.1002/2015JC011583>

Galley, R. J., Else, B. G. T., Prinsenberg, S., Babb, D. G., & Barber, D. G. (2013). Sea ice concentration, extent, age, motion and thickness in regions of proposed offshore oil and gas development near the Mackenzie Delta-Canadian Beaufort Sea. *Arctic*, 66(1), 105–116.

Gow, A. J., & Tucker, W. B. (1987). Physical properties of sea ice discharged from Fram Strait. *Science*, 236(4800), 436–439. <https://doi.org/10.1126/science.236.4800.436>

Haas, C., Pfaffling, A., Hendricks, S., Rabenstein, L., Etienne, J. L., & Rigor, I. G. (2008). Reduced ice thickness in Arctic Transpolar Drift favors rapid ice retreat. *Geophysical Research Letters*, 35(17), 1–5. <https://doi.org/10.1029/2008GL034457>

Hansen, E., Gerland, S., Granskog, M. A., Pavlova, O., Renner, A. H. H., Haapala, J., et al. (2013). Thinning of Arctic sea ice observed in Fram Strait: 1990–2011. *Journal of Geophysical Research: Oceans*, 118(10), 5202–5221. <https://doi.org/10.1002/jgrc.20393>

Hersbach, H., Bell, B., Berrisford, P., Hirahara, S., Horányi, A., Muñoz-Sabater, J., et al. (2020). The ERA5 global reanalysis. *Quarterly Journal of the Royal Meteorological Society*, 146(730), 1999–2049. <https://doi.org/10.1002/qj.3803>

Hibler, W. D., Hutchings, J. K., & Ip, C. F. (2006). Sea-ice arching and multiple flow States of Arctic pack ice. *Annals of Glaciology*, 44, 339–344. <https://doi.org/10.3189/172756406781811448>

Howell, S. E. L., Babb, D. G., Landy, J. C., & Brady, M. (2022). Multi-year sea ice conditions in the Northwest Passage: 1968–2020. *Atmosphere-Ocean*, 61(4), 1–15. <https://doi.org/10.1080/07055900.2022.2136061>

Howell, S. E. L., Babb, D. G., Landy, J. C., Moore, G. W. K., Montpetit, B., & Brady, M. (2023). A comparison of Arctic Ocean sea ice export between Nares Strait and the Canadian Arctic Archipelago. *Journal of Geophysical Research: Oceans*, 128(4), e2023JC019687. <https://doi.org/10.1029/2023JC019687>

Howell, S. E. L., & Brady, M. (2019). The dynamic response of sea ice to warming in the Canadian Arctic Archipelago. *Geophysical Research Letters*, 46(22), 13119–13125. <https://doi.org/10.1029/2019GL085116>

Jahn, A., Sterling, K., Holland, M. M., Kay, J. E., Maslanik, J. A., Bitz, C. M., et al. (2012). Late-twentieth-century simulation of Arctic sea ice and ocean properties in the CCSM4. *Journal of Climate*, 25(5), 1431–1452. <https://doi.org/10.1175/JCLI-D-11-00201.1>

Kacimi, S., & Kwok, R. (2022). Arctic snow depth, ice thickness, and volume from ICESat-2 and CryoSat-2: 2018–2021. *Geophysical Research Letters*, 49(5), 2018–2021. <https://doi.org/10.1029/2021gl097448>

Kim, Y., Min, S., Gillett, N. P., Notz, D., & Malinina, E. (2023). Observationally-constrained projections of an ice-free Arctic even under a low emission scenario. *Nature Communications*, 14(1), 3139. <https://doi.org/10.1038/s41467-023-38511-8>

Kirillov, S., Babb, D. G., Komarov, A. S., Dmitrenko, I., Ehn, J. K., Worden, E., et al. (2021). On the physical settings of ice bridge formation in Nares Strait. *Journal of Geophysical Research: Oceans*, 126(8), 1–19. <https://doi.org/10.1029/2021JC017331>

Korosov, A., Rampal, P., Toudal Pedersen, L., Saldo, R., Ye, Y., Heygster, G., et al. (2018). A new tracking algorithm for sea ice age distribution estimation. *The Cryosphere*, 12(6), 2073–2085. <https://doi.org/10.5194/tc-12-2073-2018>

- Krishfield, R. A., Proshutinsky, A., Tateyama, K., Williams, W. J., Carmack, E. C., McLaughlin, F. A., & Timmermans, M.-L. (2014). Deterioration of perennial sea ice in the Beaufort Gyre from 2003 to 2012 and its impact on the oceanic freshwater cycle. *Journal of Geophysical Research: Oceans*, *119*(2), 35–1305. <https://doi.org/10.1002/2013JC008999>
- Kruppen, T., Belter, H. J., Boetius, A., Damm, E., Haas, C., Hendricks, S., et al. (2019). Arctic warming interrupts the Transpolar Drift and affects long-range transport of sea ice and ice-rafted matter. *Scientific Reports*, *9*, 1–9. <https://doi.org/10.1038/s41598-019-41456-y>
- Kuang, H., Luo, Y., Ye, Y., Shokr, M., Chen, Z., Wang, S., et al. (2022). Arctic multiyear ice areal flux and its connection with large-scale atmospheric circulations in the winters of 2002–2021. *Remote Sensing*, *14*(15), 3742. <https://doi.org/10.3390/rs14153742>
- Kwok, R. (2004a). Annual cycles of multiyear sea ice coverage of the Arctic Ocean: 1999–2003. *Journal of Geophysical Research: Oceans*, *109*(11), 1999–2003. <https://doi.org/10.1029/2003JC002238>
- Kwok, R. (2004b). Fram Strait sea ice outflow. *Journal of Geophysical Research*, *109*(C1), C01009. <https://doi.org/10.1029/2003JC001785>
- Kwok, R. (2005). Variability of Nares Strait ice flux. *Geophysical Research Letters*, *32*(24), 1–4. <https://doi.org/10.1029/2005GL024768>
- Kwok, R. (2006). Exchange of sea ice between the Arctic Ocean and the Canadian Arctic Archipelago. *Geophysical Research Letters*, *33*(16), 1–5. <https://doi.org/10.1029/2006GL027094>
- Kwok, R. (2007). Near zero replenishment of the Arctic multiyear sea ice cover at the end of 2005 summer. *Geophysical Research Letters*, *34*(5), 1–6. <https://doi.org/10.1029/2006GL028737>
- Kwok, R. (2009). Outflow of Arctic Ocean sea ice into the Greenland and Barent Seas: 1979–2007. *Journal of Climate*, *22*(9), 2438–2457. <https://doi.org/10.1175/2008JCLI2819.1>
- Kwok, R. (2015). Sea ice convergence along the Arctic coasts of Greenland and the Canadian Arctic Archipelago: Variability and extremes (1992–2014). *Geophysical Research Letters*, *42*(18), 1–8. <https://doi.org/10.1002/2015GL065462>
- Kwok, R. (2018). Arctic sea ice thickness, volume, and multiyear ice coverage: Losses and coupled variability (1958–2018). *Environmental Research Letters*, *13*(10), 105005. <https://doi.org/10.1088/1748-9326/aae3ec>
- Kwok, R., & Cunningham, G. F. (2010). Contribution of melt in the Beaufort Sea to the decline in Arctic multiyear sea ice coverage: 1993–2009. *Geophysical Research Letters*, *37*(20), 1–5. <https://doi.org/10.1029/2010GL044678>
- Kwok, R., & Cunningham, G. F. (2015). Variability of Arctic sea ice thickness and volume from CryoSat-2. *Philosophical Transactions of the Royal Society A*, *373*, 2045. <https://doi.org/10.1098/rsta.2014.0157>
- Kwok, R., Cunningham, G. F., Wensnahan, M., Rigor, I. G., Zwally, H. J., & Yi, D. (2009). Thinning and volume loss of the Arctic Ocean sea ice cover: 2003–2008. *Journal of Geophysical Research: Oceans*, *114*(7), 1–16. <https://doi.org/10.1029/2009JC005312>
- Kwok, R., Maslowski, W., & Laxon, S. W. (2005). On large outflows of Arctic sea ice into the Barents Sea. *Geophysical Research Letters*, *32*(22), 1–5. <https://doi.org/10.1029/2005GL024485>
- Kwok, R., Pedersen, L. T., Gudmandsen, P., & Pang, S. S. (2010). Large sea ice outflow into the Nares Strait in 2007. *Geophysical Research Letters*, *37*(3). <https://doi.org/10.1029/2009GL041872>
- Kwok, R., & Rothrock, D. A. (2009). Decline in Arctic sea ice thickness from submarine and ICESat records: 1958–2008. *Geophysical Research Letters*, *36*(15), 1–5. <https://doi.org/10.1029/2009GL039035>
- Kwok, R., Spreen, G., & Pang, S. (2013). Arctic sea ice circulation and drift speed: Decadal trends and ocean currents. *Journal of Geophysical Research: Oceans*, *118*(5), 2408–2425. <https://doi.org/10.1002/jgrc.20191>
- Lindsay, R. W., & Zhang, J. (2005). The thinning of Arctic sea ice, 1988–2003: Have we passed a tipping point? *Journal of Climate*, *18*(22), 4879–4894. <https://doi.org/10.1175/JCLI3587.1>
- Lindsay, R. W., Zhang, J., Schweiger, A., Steele, M., & Stern, H. (2009). Arctic sea ice retreat in 2007 follows thinning trend. *Journal of Climate*, *22*(1), 165–176. <https://doi.org/10.1175/2008JCLI2521.1>
- Mahoney, A. R., Hutchings, J. K., Eicken, H., & Haas, C. (2019). Changes in the thickness and circulation of multiyear ice in the Beaufort Gyre determined from Pseudo-Lagrangian methods from 2003–2015. *Journal of Geophysical Research: Oceans*, *124*(8), 5618–5633. <https://doi.org/10.1029/2018JC014911>
- Mallett, R. D. C., Stroeve, J. C., Cornish, S. B., Crawford, A. D., Lukovich, J. V., Serreze, M. C., et al. (2021). Record winter winds in 2020/21 drove exceptional Arctic sea ice transport. *Communications Earth & Environment*, *2*(1), 17–22. <https://doi.org/10.1038/s43247-021-00221-8>
- Maslanik, J. A., Fowler, C., Stroeve, J. C., Drobot, S., Zwally, J., Yi, D., & Emery, W. (2007). A younger, thinner Arctic ice cover: Increased potential for rapid, extensive sea-ice loss. *Geophysical Research Letters*, *34*(24), 2004–2008. <https://doi.org/10.1029/2007GL032043>
- Maslanik, J. A., Stroeve, J. C., Fowler, C., & Emery, W. (2011). Distribution and trends in Arctic sea ice age through spring 2011. *Geophysical Research Letters*, *38*(13), 2–7. <https://doi.org/10.1029/2011GL047735>
- Meier, W. N., Perovich, D. K., Farrell, S. L., Haas, C., Hendricks, S., Petty, A. A., et al. (2021). Sea Ice [in “State of the Climate in 2021”]. <https://doi.org/10.25923/y2wd-fm85>
- Meier, W. N., & Stewart, J. S. (2023). Early EASE-GRID Sea Ice Age, 1978–1983 (Version 4.1_early) [Dataset]. Zenodo. <https://doi.org/10.5281/ZENODO.7659077>
- Melling, H. (2002). Sea ice of the northern Canadian Arctic Archipelago. *Journal of Geophysical Research*, *107*(C11), 3181. <https://doi.org/10.1029/2001JC001102>
- Meredith, M., Sommerkorn, M., Cassotta, S., Derksen, C., Ekaykin, A., Hollowed, A., et al. (2019). Polar regions. In H.-O. Portner, D. C. Roberts, V. Masson-Delmotte, P. Zhai, M. Tignor, E. Poloczanska, et al. (Eds.), *IPCC Special Report on the Ocean and Cryosphere in a Changing Climate* (p. 118).
- Moore, G. W. K., Howell, S. E. L., & Brady, M. (2021). First observations of a transient polynya in the Last Ice Area north of Ellesmere Island. *Geophysical Research Letters*, *48*(17), e2021GL095099. <https://doi.org/10.1029/2021GL095099>
- Moore, G. W. K., Howell, S. E. L., Brady, M., Xu, X., & McNeil, K. (2021). Anomalous collapses of Nares Strait ice arches leads to enhanced export of Arctic sea ice. *Nature Communications*, *12*(1), 1–8. <https://doi.org/10.1038/s41467-020-20314-w>
- Moore, G. W. K., Schweiger, A., Zhang, J., & Steele, M. (2019). Spatiotemporal variability of sea ice in the Arctic’s Last Ice Area. *Geophysical Research Letters*, *46*(20), 11237–11243. <https://doi.org/10.1029/2019GL083722>
- Nghiem, S. V., Chao, Y., Neumann, G., Li, P., Perovich, D. K., Street, T., & Clemente-Colón, P. (2006). Depletion of perennial sea ice in the East Arctic Ocean. *Geophysical Research Letters*, *33*(17), 1–6. <https://doi.org/10.1029/2006GL027198>
- Nghiem, S. V., Neumann, G., Rigor, I. G., Clemente-Colón, P., & Perovich, D. K. (2011). Arctic perennial sea ice crash of the 2000s and its impacts. In *BIONATURE 2011 Second International Conference Bioenvironment, Biodiversity Renewable Energies, March 2007* (pp. 38–42).
- Nghiem, S. V., Rigor, I. G., Perovich, D. K., Clemente-Colón, P., Weatherly, J. W., & Neumann, G. (2007). Rapid reduction of Arctic perennial sea ice. *Geophysical Research Letters*, *34*(19), 1–6. <https://doi.org/10.1029/2007GL031138>
- Notz, D. (2009). The future of ice sheets and sea ice: Between reversible retreat and unstoppable loss. *Proceedings of the National Academy of Sciences of the United States of America*, *106*(49), 20590–20595. <https://doi.org/10.1073/pnas.0902356106>

- Notz, D., & SIMIP Community. (2020). Arctic sea ice in CMIP6. *Geophysical Research Letters*, 47(10), e2019GL086749. <https://doi.org/10.1029/2019gl086749>
- Perovich, D. K., & Polashenski, C. (2012). Albedo evolution of seasonal Arctic sea ice. *Geophysical Research Letters*, 39(8), 1–6. <https://doi.org/10.1029/2012GL051432>
- Perovich, D. K., Richeter-Menge, J. A., Jones, K. F., & Light, B. (2008). Sunlight, water, and ice: Extreme Arctic sea ice melt during the summer of 2007. *Geophysical Research Letters*, 35(11), 2–5. <https://doi.org/10.1029/2008GL034007>
- Petty, A. A., Holland, M. M., Bailey, D. A., & Kurtz, N. T. (2018). Warm Arctic, increased winter sea ice growth? *Geophysical Research Letters*, 45(23), 12922–12930. <https://doi.org/10.1029/2018GL079223>
- Petty, A. A., Keeney, N., Cabaj, A., Kushner, P., & Bagnardi, M. (2023). Winter Arctic sea ice thickness from ICESat-2: Upgrades to freeboard and snow loading estimates and an assessment of the first three winters of data collection. *The Cryosphere*, 17(1), 127–156. <https://doi.org/10.5194/tc-17-127-2023>
- Pfirman, S., Haxby, W. F., Colony, R., & Rigor, I. G. (2004). Variability in Arctic sea ice drift. *Geophysical Research Letters*, 31(16), 1–4. <https://doi.org/10.1029/2004GL020063>
- Pizzolato, L., Howell, S. E. L., Derksen, C., Dawson, J., & Copland, L. (2014). Changing sea ice conditions and marine transportation activity in Canadian Arctic waters between 1990 and 2012. *Climate Change*, 123(2), 161–173. <https://doi.org/10.1007/s10584-013-1038-3>
- Rampal, P., Weiss, J., & Marsan, D. (2009). Positive trend in the mean speed and deformation rate of Arctic sea ice, 1979–2007. *Journal of Geophysical Research: Oceans*, 114(5), 1–14. <https://doi.org/10.1029/2008JC005066>
- Regan, H. C., Rampal, P., Ólason, E., Boutin, G., & Korosov, A. (2023). Modelling the evolution of Arctic multiyear sea ice over 2000–2018. *The Cryosphere*, 17(5), 1–28. <https://doi.org/10.5194/tc-17-1873-2023>
- Ricker, R., Girard-Arduin, F., Krumpen, T., & Lique, C. (2018). Satellite-derived sea ice export and its impact on Arctic ice mass balance. *The Cryosphere*, 12(9), 3017–3032. <https://doi.org/10.5194/tc-12-3017-2018>
- Ricker, R., Hendricks, S., Girard-Arduin, F., Kaleschke, L., Lique, C., Tian-Kunze, X., et al. (2017). Satellite-observed drop of Arctic sea ice growth in winter 2015–2016. *Geophysical Research Letters*, 44(7), 3236–3245. <https://doi.org/10.1002/2016GL072244>
- Ricker, R., Kauker, F., Schweiger, A., Hendricks, S., Zhang, J., & Paul, S. (2021). Evidence for an increasing role of ocean heat in Arctic winter sea ice growth. *Journal of Climate*, 34(13), 5215–5227. <https://doi.org/10.1175/JCLI-D-20-0848.1>
- Rigor, I. G., & Wallace, J. M. (2004). Variations in the age of Arctic sea-ice and summer sea-ice extent. *Geophysical Research Letters*, 31(9), 2–5. <https://doi.org/10.1029/2004GL019492>
- Rigor, I. G., Wallace, J. M., & Colony, R. L. (2002). Response of sea ice to the Arctic Oscillation. *Journal of Climate*, 15(18), 2648–2663. [https://doi.org/10.1175/1520-0442\(2002\)015<2648:ROSITT>2.0.CO;2](https://doi.org/10.1175/1520-0442(2002)015<2648:ROSITT>2.0.CO;2)
- Rothrock, D. A., Yu, Y., & Maykut, G. A. (1999). Thinning of the Arctic sea-ice cover. *Geophysical Research Letters*, 26(23), 3469–3472. <https://doi.org/10.1029/1999GL010863>
- Schweiger, A. J., Steele, M., Zhang, J., Moore, G. W. K., & Laidre, K. L. (2021). Accelerated sea ice loss in the Wandel Sea points to a change in the Arctic's Last Ice Area. *Communications Earth & Environment*, 2(1), 122. <https://doi.org/10.1038/s43247-021-00197-5>
- Shokr, M., Lambe, A., & Agnew, T. (2008). A new algorithm (ECICE) to estimate ice concentration from remote sensing observations: An application to 85-GHz passive microwave data. *IEEE Transactions on Geoscience and Remote Sensing*, 46(12), 4104–4121. <https://doi.org/10.1109/TGRS.2008.2000624>
- Smedsrud, L. H., Halvorsen, M. H., Stroeve, J. C., Zhang, R., & Kloster, K. (2017). Fram Strait sea ice export variability and September Arctic sea ice extent over the last 80 years. *The Cryosphere*, 11(1), 65–79. <https://doi.org/10.5194/tc-11-65-2017>
- Stroeve, J. C., & Notz, D. (2018). Changing state of Arctic sea ice across all seasons. *Environmental Research Letters*, 13(10), 103001. <https://doi.org/10.1088/1748-9326/aade56>
- Stroeve, J. C., Schroder, D., Tsamados, M., & Feltham, D. (2018). Warm winter, thin ice? *The Cryosphere*, 12(5), 1791–1809. <https://doi.org/10.5194/tc-12-1791-2018>
- Sumata, H., de Steur, L., Divine, D. V., Granskog, M. A., & Gerland, S. (2023). Regime shift in Arctic Ocean sea ice thickness. *Nature*, 615(7952), 443–449. <https://doi.org/10.1038/s41586-022-05686-x>
- Sumata, H., de Steur, L., Gerland, S., Divine, D. V., & Pavlova, O. (2022). Unprecedented decline of Arctic sea ice outflow in 2018. *Nature Communications*, 13(1), 1747. <https://doi.org/10.1038/s41467-022-29470-7>
- Sumata, H., Lavergne, T., Girard-Arduin, F., Kimura, N., Tschudi, M., Kauker, F., et al. (2014). An intercomparison of Arctic ice drift products to deduce uncertainty estimates. *Journal of Geophysical Research: Oceans*, 119(8), 4887–4921. <https://doi.org/10.1002/2013JC009724>
- Thomas, D. R., & Rothrock, D. A. (1993). The Arctic Ocean ice balance: A Kalman smoother estimate. *Journal of Geophysical Research*, 98(C6), 10053–10067. <https://doi.org/10.1029/93JC00139>
- Tilling, R. L., Ridout, A., Shepherd, A., & Wingham, D. J. (2015). Increased Arctic sea ice volume after anomalously low melting in 2013. *Nature Geoscience*, 8, 643–646. <https://doi.org/10.1038/NGEO2489>
- Tschudi, M. A., Meier, W. N., Stewart, J. S., Fowler, C., & Maslanik, J. A. (2019a). EASE-Grid Sea Ice Age, Version 4 [Dataset]. <https://doi.org/10.5067/UTAV7490FEPB>
- Tschudi, M. A., Meier, W. N., Stewart, J. S., Fowler, C., & Maslanik, J. A. (2019b). Polar Pathfinder daily 25 km EASE-Grid Sea Ice Motion Vectors, Version 4 [Dataset]. <https://doi.org/10.5067/INAWUW07QH7B>
- Tschudi, M. A., Stroeve, J. C., & Stewart, J. S. (2016). Relating the age of Arctic sea ice to its thickness, as measured during NASA's ICESat and IceBridge campaigns. *Remote Sensing*, 8(6), 457. <https://doi.org/10.3390/rs8060457>
- Vincent, R. F. (2019). A study of the north water polynya ice arch using four decades of satellite data. *Scientific Reports*, 9(1), 1–12. <https://doi.org/10.1038/s41598-019-56780-6>
- Wang, Y., Bi, H., & Liang, Y. (2022). A satellite-observed substantial decrease in multiyear ice area export through the Fram Strait over the last decade. *Remote Sensing*, 14(11), 2562. <https://doi.org/10.3390/rs14112562>
- Ye, Y., Luo, Y., Sun, Y., Shokr, M., Aaboe, S., Girard-Arduin, F., et al. (2023). Inter-comparison and evaluation of Arctic sea ice type products. *The Cryosphere*, 17(1), 279–308. <https://doi.org/10.5194/tc-17-279-2023>